Table 1
Antigenic properties of rgAnhui-H5N1 vaccine virus and HPAIVs.

Viruses	Genetic clade	Post-infection ferret sera		
		JWE	rgAnhui	Laos
VN	1	<10	20	40
Indo	2.1.3	80	1280	160
Tk	2.2	160	80	40
JWE	2.3.4	**320**	320	320
rgAnhui	2.3.4	160	**1280**	1280
Laos	2.3.4	160	1280	**1280**
Myan	2.3.4	40	160	320

Bold type refers to homologous HI titers for indicated viruses.

2.6. The survival curve was compared using Log-rank test

Student's *t*-test or Mann–Whitney U test was performed to compare viral HA-specific IgG1 and IgG2a antibodies against various virus strains.

All statistical analyses, except for Steel's method, were performed with PASW statistical software (IBM Japan Ltd., Tokyo, Japan) and the *p*-value of each comparison under 0.05 was regarded as statistically significant difference.

3. Results

3.1. Antigenic properties of rgAnhui vaccine virus and H5N1 HPAIVs

First, we analyzed the antigenic properties of all viruses used in this study by performing HI assay with post-infection ferret antisera. As shown in Table 1, rgAnhui, Laos and JWE viruses of clade 2.3.4 exhibited similar antigenicity, as indicated by HI titers within 4-fold of the HI titers for each homologous antiserum. Myan virus, however, showed 8-fold lower HI titers against anti-rgAnhui and anti-JWE sera, and 4-fold lower HI titer against anti-Laos serum, indicating that the virus was antigenically different from rgAnhui and the two clade 2.3.4 viruses, although the Myan virus also belongs to clade 2.3.4. With respect to the heterologous clade viruses, the HI titer of Indo (clade 2.1.3) virus against anti-rgAnhui serum was the same as the homologous HI titer, whereas VN (clade 1) and Tk (clade 2.2) viruses exhibited 64-fold and 16-fold lower HI titers against anti-rgAnhui serum, respectively. Thus, HI assay clearly indicated that VN and Tk viruses were antigenically different from rgAnhui vaccine virus, while Indo virus was closely related to the vaccine virus, despite the heterologous genetic clade.

3.2. Induction of virus-neutralizing antibodies in sera from vaccinated mice

In order to investigate the immunogenicity of the rgAnhui vaccine, mice were subcutaneously vaccinated with a high (3 μg HA) or low (0.3 μg HA) doses of vaccine antigen with or without alum. On day 42 (21 days after the 2nd vaccination), sera were collected from vaccinated mice and virus-neutralizing antibody titers against various clades of wild-type H5N1 HPAIVs were measured (Fig. 1). JWE was used as a homologue of the wild-type virus in rgAnhui vaccine, as wild-type A/Anhui/01/2005 was not available and JWE virus is antigenically similar (Table 1). The virus-neutralizing antibody titer against homologous JWE virus was correlated with both the antigen dose and the presence of alum. Mice vaccinated with 0.3 μg HA antigen with adjuvant produced almost the same level of serum virus-neutralizing antibody as that induced by vaccination with 3 μg HA antigen without adjuvant, indicating that one-tenth the amount of vaccine antigen could be used with addition of alum. Similar reactivity occurred against the Laos strain, which is from

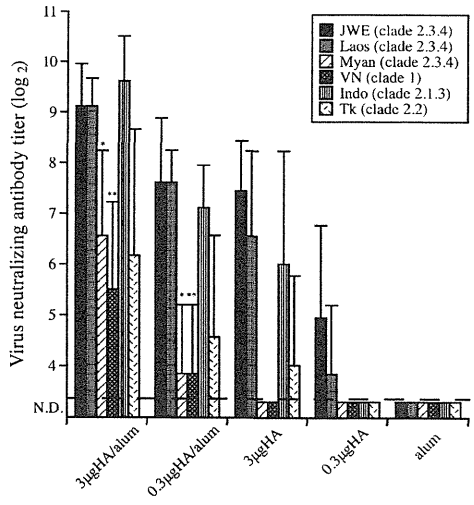

Fig. 1. Virus-neutralizing antibody titers in sera from vaccinated mice. Mice were vaccinated twice with H5N1 rgAnhui vaccine (clade 2.3.4) at a 3-week interval and with or without alum. On day 21 after the second vaccination, sera were collected, and the virus-neutralizing antibody titers against various clades (2.3.4, 1, 2.1.3 and 2.2) of H5N1 viruses were measured. Each bar represents the mean titer of virus-neutralizing antibodies, and error bars represent standard deviations. The dashed line represents the detection limit. $^{*}p < 0.05$ for comparison with JWE or Laos strain and $p > 0.05$ for comparison with VN strain using Steel's method. $^{**}p < 0.05$ for comparison with JWE, Laos or Indo strain and $p > 0.05$ for comparison with Tk strain using Steel's method.

the same clade (2.3.4) and is antigenically similar to the rgAnhui vaccine virus (Table 1). In contrast, the antibody reactivity to an antigenic variant virus of clade 2.3.4, the Myan strain (Table 1), was significantly weaker than that of JWE and Laos strain ($p < 0.05$, Steel's method for multiple comparison), and the titer was similar to that against heterologous clade 1 virus, the VN strain. Furthermore, virus-neutralizing antibodies against the Myan strain were not detectable at any antigen dose with non-adjuvanted vaccine.

In order to assess cross-reactivity against heterologous clade viruses, virus-neutralizing antibody titers against the VN strain (clade 1), Indo strain (clade 2.1.3) and Tk strain (clade 2.2) were also measured (Fig. 1). Mice vaccinated with adjuvanted vaccine showed a high level of cross-reactive virus-neutralizing antibodies against Indo virus and an intermediate level of virus-neutralizing antibody against Tk virus. These cross-reactive virus-neutralizing antibodies were also detected by vaccination with high-dose non-adjuvanted vaccine. Virus-neutralizing antibody against VN strain was induced only in mice receiving vaccine antigen with adjuvant. Anti-VN virus-neutralizing antibody titers were similar to those of anti-Tk, but were significantly lower than anti-JWE, -Laos or -Indo antibody titers ($p < 0.05$, Steel's method for multiple comparison).

3.3. Protective efficacy of inactivated rgAnhui vaccine against lethal-dose infections with homologous clade H5N1 HPAIVs

The protective efficacy of rgAnhui vaccine was evaluated in mice that were subcutaneously vaccinated twice, as outlined in Fig. 1. On day 42, mice were anesthetized and intranasally infected with a lethal dose (20 × MLD_{50}) of homologous clade viruses (JWE, Laos or Myan). All mice vaccinated with either dose of antigen with or without adjuvant survived the lethal-dose infection (Fig. 2). Moreover, none of the infected mice lost a significant amount of weight during the 14-day observation period (Fig. 3). In contrast, the weight of control mice (inoculated with alum adjuvant alone) began to decrease at 4–6 days after HPAIV infection, and all control mice were dead by day 10 after infection (Figs. 2 and 3).

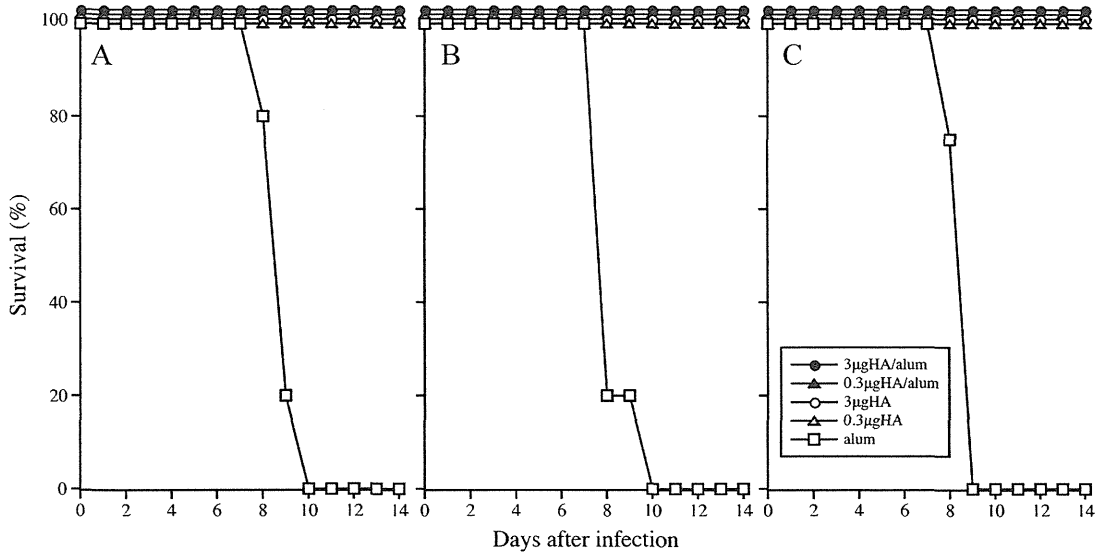

Fig. 2. Survival rate of vaccinated mice after lethal infection with homologous clade 2.3.4 viruses. Five mice in each group were vaccinated twice with H5N1 rgAnhui vaccine (with or without alum) at a 3-week interval (●, 3 μg HA with alum; ▲, 0.3 μg HA with alum; ○, 3 μg HA; △, 0.3 μg HA; □, alum). On day 21 after the second vaccination, mice were anesthetized and inoculated intranasally with a lethal dose of homologous clade JWE (A), Laos (B) or Myan (C) strain, and their survival was monitored for 2 weeks.

3.4. Cross-protective efficacy of inactivated rgAnhui vaccine against lethal-dose infections with heterologous clade H5N1 HPAIVs

Next, we examined the cross-protective efficacy of rgAnhui vaccine by challenge infection with 20 × MLD_{50} of various heterologous clades of H5N1 HPAIVs. After clade 1 VN virus infection, only 20% of mice vaccinated with a low dose (0.3 μg HA) of non-adjuvanted vaccine survived (Fig. 4A), and severe weight loss similar to that of the control mice occurred until day 9 after virus infection (Fig. 5A). However, the survival rate increased to 80% when mice were vaccinated with the same dose of adjuvanted vaccine (Fig. 4A). These mice lost some weight during days 3–7, after which they returned to a normal weight (Fig. 5A). At a high dose (3 μg HA) of adjuvanted vaccine, all mice survived and no significant weight loss was observed, whereas one mouse was dead at day 16 by vaccination with non-adjuvanted vaccine (Fig. 4A).

In a challenge infection with Indo virus (clade 2.1.3) (Figs. 4B and 5B), all vaccinated mice survived without significant weight loss, regardless of the dose and presence or absence of adjuvant, with the exception of mice vaccinated with 0.3 μg HA non-adjuvanted vaccine; these mice had a weight loss of approximately 10% during days 4–8, after which their weight recovered. In contrast, the control mice lost weight starting at 3 days after virus infection, and all control mice were dead by day 9 after infection (Fig. 5B).

On challenge infection with Tk (clade 2.2) virus (Fig. 4C), the survival rate of mice vaccinated with 0.3 μg HA non-adjuvanted

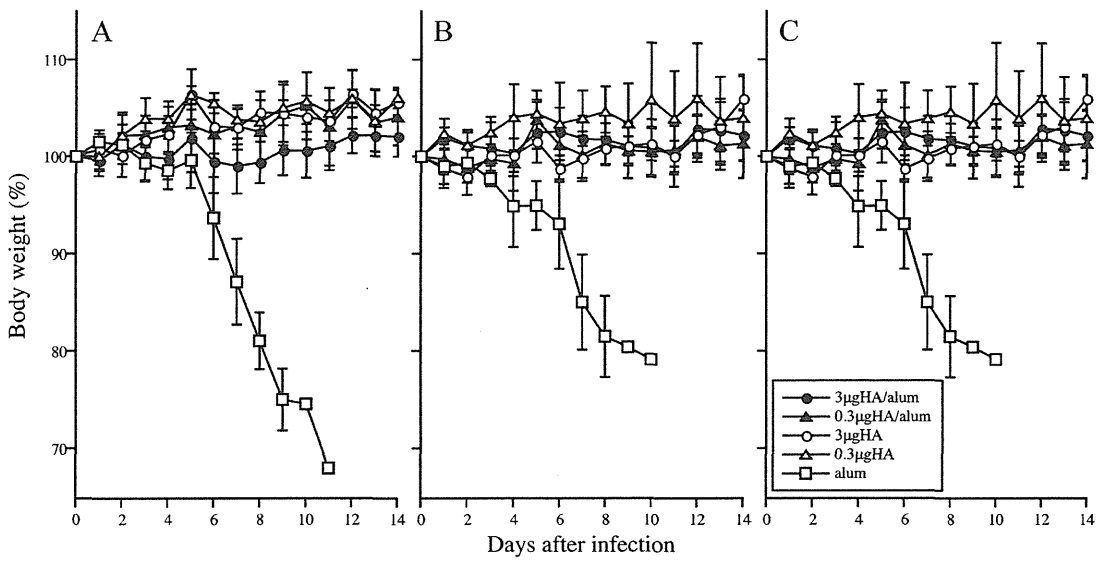

Fig. 3. Weight changes in vaccinated mice after lethal infection with homologous clade 2.3.4 viruses. Five mice in each group were vaccinated twice with H5N1 rgAnhui vaccine (with or without alum) at a 3-week interval (●, 3 μg HA with alum; ▲, 0.3 μg HA with alum; ○, 3 μg HA; △, 0.3 μg HA; □, alum). On day 21 after the second vaccination, mice were anesthetized and inoculated intranasally with a lethal dose of homologous clade JWE (A), Laos (B) or Myan (C) strain, and their weight was monitored for 2 weeks. Weight is expressed as a percentage of weight on day 0. Data represent the mean weight of mice, and error bars represent standard deviations.

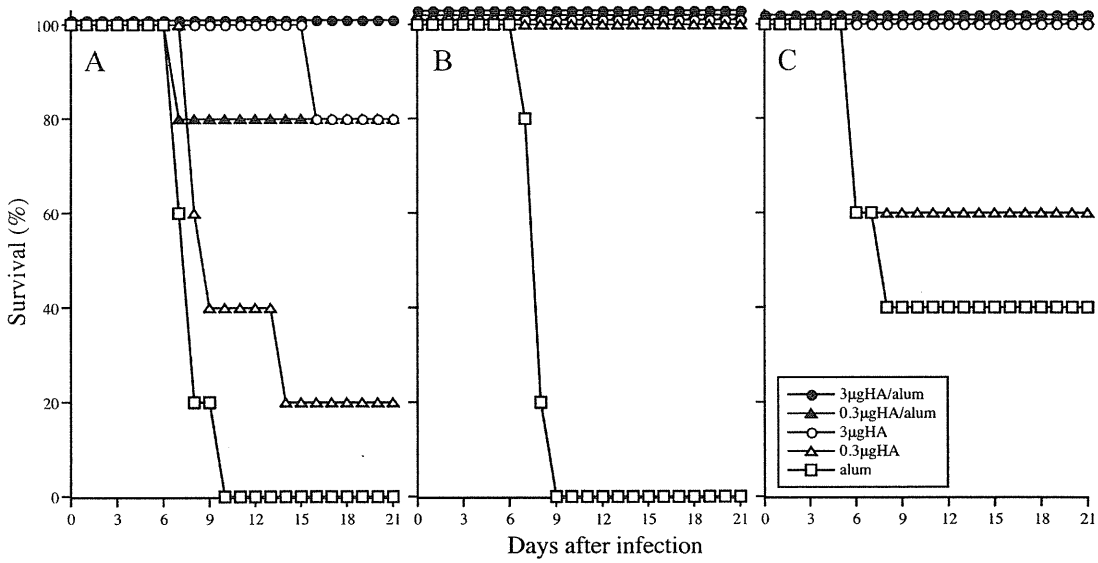

Fig. 4. Survival rate of vaccinated mice after lethal infection with heterologous clade viruses. Five mice in each group were vaccinated twice with H5N1 rgAnhui vaccine (clade 2.3.4) at a 3-week interval and with or without alum (●, 3 μg HA with alum; ▲, 0.3 μg HA with alum; ○, 3 μg HA; △, 0.3 μg HA; □, alum). On day 21 after the second vaccination, mice were anesthetized and inoculated intranasally with a lethal dose of heterologous clade 1 VN (A), clade 2.1.3 Indo (B) or clade 2.2 Tk (C) strain, and their survival was monitored for 3 weeks.

vaccine was 60%, which was not significantly higher than that of the control mice (Log-rank (Mantel-Cox) test, $p = 0.582$). However, the survival rate was 100% with the addition of adjuvant. At a high dose of vaccine antigen, all mice survived, regardless of the presence or absence of adjuvant. However, unlike other clades of challenge virus, Tk infection caused weight loss in all vaccinated mice starting at 1–2 days after infection (Fig. 5C). The severity of weight loss depended on the vaccine antigen dose (0.3 μg HA antigen was associated with more marked weight loss than 3 μg HA antigen), but all mice returned to a normal weight by day 14. Moreover, recovery from weight loss occurred earlier in the mice that received adjuvanted vaccine as compared to the non-adjuvanted vaccine at the same vaccine antigen dose (Fig. 5C).

3.5. Detection of viral HA-specific IgG1 and IgG2a antibodies in sera from vaccinated mice

HA protein from influenza virus is the major antigen for induction of protective antibodies. Alum is thought to enhance the induction of antigen-specific IgG1 antibody responses [26,27]. It has also been reported that virus-specific IgG2a antibodies are induced by live influenza virus infection and are important to

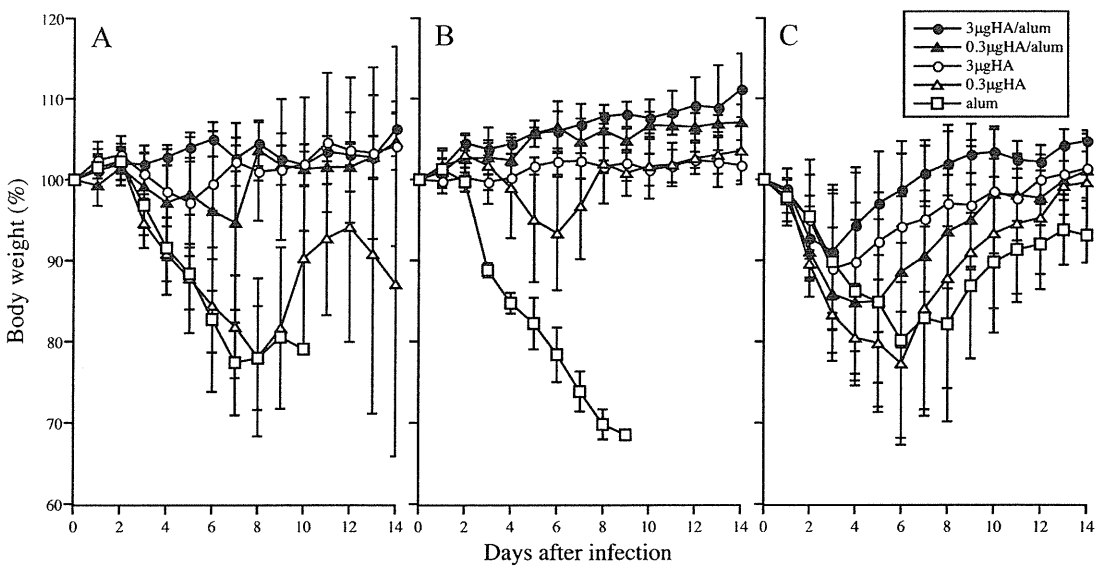

Fig. 5. Weight changes in vaccinated mice after lethal infection with heterologous clade viruses. Five mice in each group were vaccinated twice with H5N1 rgAnhui vaccine (clade 2.3.4) at a 3-week interval and with or without alum (●, 3 μg HA with alum; ▲, 0.3 μg HA with alum; ○, 3 μg HA; △, 0.3 μg HA; □, alum). On day 21 after the second vaccination, mice were anesthetized and inoculated intranasally with a lethal dose of heterologous clade 1 VN (A), clade 2.1.3 Indo (B) or clade 2.2 Tk (C) strain, and their weight was monitored for 2 weeks. Weight is expressed as a percentage of weight on day 0. Data represent the mean weight of mice, and error bars represent standard deviations.

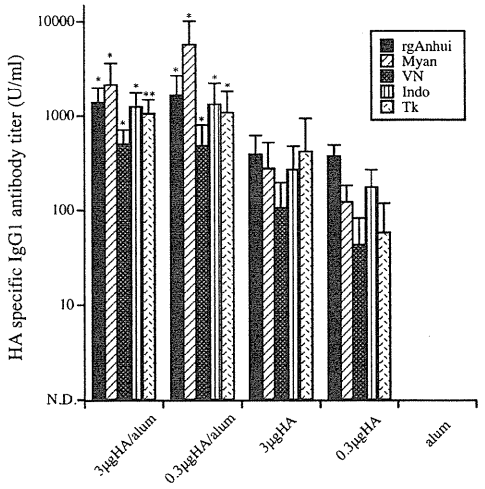

Fig. 6. Viral HA-specific IgG1 antibody titers in sera from vaccinated mice. Mice were vaccinated twice at a 3-week interval and with or without alum. On day 21 after the second vaccination, sera were collected, and viral HA-specific IgG1 antibody titers against various clades of H5N1 viruses were measured by ELISA. Each bar represents the mean value of viral HA-specific IgG1 antibody titers, and error bars represent standard deviations. *$p < 0.05$ for comparison against each vaccine antigen only using Student's *t*-test. **$p < 0.05$ for comparison against each vaccine antigen only using Mann–Whitney *U* test.

antibody-mediated protection against influenza A virus infection [28,29]. Thus, we used ELISA to measure HA-specific IgG1 and IgG2a antibody titers in the sera of vaccinated mice. Sera subjected to ELISA were the same as those used for the titration of virus-neutralizing antibodies.

All vaccinated mice developed HA-specific IgG1 and IgG2a antibodies (Figs. 6 and 7). These antibodies could not be detected in the sera of control mice. Alum significantly enhanced the induction of cross-reactive IgG1 ($p < 0.05$, Student's *t*-test or Mann–Whitney *U* test) and IgG2a ($p < 0.01$, Student's *t*-test or Mann–Whitney *U* test) antibodies against all test HAs from H5N1 viruses belonging to different clades. In particular, IgG1 antibody levels at a low antigen

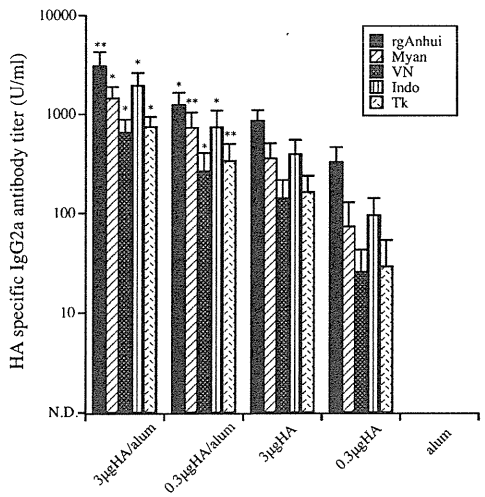

Fig. 7. Viral HA-specific IgG2a antibody titers in sera from vaccinated mice. Mice were vaccinated twice at a 3-week interval and with or without alum. On day 21 after the second vaccination, sera were collected, and viral HA-specific IgG2a antibody titers against various clades of H5N1 viruses were measured by ELISA. Each bar represents the mean value for viral HA-specific IgG2a antibody titers, and error bars represent standard deviation. *$p < 0.01$ for comparison against each vaccine antigen only using Student's *t*-test. **$p < 0.01$ for comparison against each vaccine antigen only using Mann–Whitney *U* test.

dose were efficiently enhanced by addition of adjuvant, and IgG1 antibody titers at the low antigen dose were as high against all test viral HAs as those at the high antigen dose (Fig. 6). It is noteworthy that IgG1 antibody titers against the HA from the antigenic variant Myan virus were higher, but not significantly so ($p = 0.055$, Student's *t*-test), than those against the HA from rgAnhui vaccine virus in the sera of mice vaccinated with adjuvanted vaccine (Fig. 6), although the virus-neutralizing antibody titer against Myan virus was significantly lower than that against JWE virus ($p < 0.05$, Steel's method for multiple comparison), and was as low as that against clade 1 virus VN (Fig. 1). Similarly, high levels of IgG2a antibodies against Myan and VN viruses were detected by ELISA.

4. Discussion

In the present study, we evaluated the vaccine efficacy of rgAnhui virus (clade 2.3.4) with respect to immunogenicity and cross-protection against viruses of homologous and heterologous genetic clades, including antigenic variants. To assess immunogenicity, we detected virus-neutralizing antibody rather than HI antibody, as in our previous mouse model study of H5N1 vaccines, HI antibody was not detected after vaccination at the highest dose (2 μg HA) of adjuvanted vaccine, while sufficient levels of virus-neutralizing antibody were detected in many cases [13]. Furthermore, virus-neutralizing assay is a hallmark for assessing the immunogenicity of H5N1 vaccines due to its higher sensitivity. In the present mouse model experiments, vaccination with 0.3 μg HA enabled the production of virus-neutralizing antibodies against homologous clade 2.3.4 viruses, except for the antigenic variant Myan virus (Fig. 1).

As expected and as reported previously [13,15], the addition of alum to 0.3 μg HA markedly increased antibody levels to levels similar to those induced by vaccination with 3 μg HA antigen. Furthermore, these antibodies were also able to neutralize homologous Myan and heterologous VN strains, and were not observed in mice receiving 3 μg HA antigen without adjuvant. Thus, serum antibodies induced by 0.3 μg HA antigen with alum were able to neutralize all test viruses in clades 1, 2.1.3 and 2.2, as well as homologous clade 2.3.4, including Myan virus. These data clearly indicate that vaccine formulations with alum allow 10-times less vaccine antigen to be used in our mouse model.

Although it has been reported that addition of alum to H5N1 vaccine did not enhance immunogenicity in a clinical study [17], non-adjuvanted H5N1 vaccines required large amounts of vaccine antigen to induce serum antibodies that meet the evaluation criteria for vaccines by the Committee for Proprietary Medicinal Products (CPMP) [12]. The strategy of vaccine antigen sparing is crucial for the creation of a national stockpile of pre-pandemic H5N1 vaccines, as manufacturers have limited vaccine production capacity. Moreover, in our unpublished clinical trials of attenuated and inactivated H5N1 vaccine in 1997, 15 μg HA antigen from split and whole virion vaccines without adjuvant failed to elicit any detectable level of neutralizing antibodies in the sera of vaccine recipients, which led us to the conclusion that an adjuvanted formulation is necessary for H5N1 vaccines. Consequently, the use of alum or other recently approved oil-in-water adjuvants, such as MF59 [17] and AS03 [18], is the most promising and realistic H5N1 vaccine strategy for pandemic preparedness.

In homologous genetic clade 2.3.4, the neutralizing antibody titers induced by rgAnhui vaccine were high against JWE and Laos viruses, but were significantly lower against Myan virus (Fig. 1). Based on antigenic analysis by HI test, JWE and Laos viruses were antigenically related to rgAnhui virus, but the Myan virus differed from the rgAnhui virus (Table 1) through substitution of two amino acids at antigenic site B of the HA protein (data not shown). However, such low cross-reactivity against the Myan virus did not

correlate with the survival rate and weight loss after lethal challenge with Myan virus; all vaccinated mice, regardless of antigen dose and presence or absence of adjuvant, survived without significant weight loss, similarly to mice exposed to other clade 2.3.4 viruses (Figs. 2 and 3).

The protection observed in vaccinated mice should be mediated by virus-specific antibodies, particularly virus-neutralizing and/or viral HA-specific antibodies, as formalin-inactivated viral antigens and alum itself cannot induce cellular immunity [16,30–32]. In fact, on ELISA, the HA-specific IgG1/IgG2a antibodies against Myan virus were markedly elicited with similar levels as homologous vaccine-like virus by non-adjuvanted rgAnhui vaccination (Figs. 6 and 7), while virus-neutralizing antibodies against Myan virus could not be detected (Fig. 1). Moreover, Lu et al. [33] reported that mice vaccinated and survived from following lethal virus challenge did not always possess detectable levels of virus-neutralizing antibodies against challenge virus. It is therefore possible that the undetectable levels of neutralizing antibody induced by vaccination were sufficient to provide protection from the homologous clade of the Myan virus.

Among heterologous clade viruses, virus-neutralizing titers, survival rate and antigenic differences were well correlated. Indo virus (clade 2.1.3) exhibited antigenic similarity to rgAnhui virus on HI test (Table 1) and was well neutralized by antibodies induced by rgAnhui vaccine, similarly to homologous clade 2.3.4 viruses (Fig. 1), and all vaccinated mice survived (Fig. 4B). The results suggest that rgAnhui vaccine sufficiently neutralized Indo-like viruses in clade 2.1.3. On the other hand, rgAnhui vaccination at a low (0.3 μg HA) dose without adjuvant was less effective against clade 1 VN virus, as only 20% of mice challenged with VN virus survived, although the survival rate increased to 80% with addition of adjuvant (Fig. 4A). Such decreased cross-protective efficacy when compared with Indo and Myan viruses, particularly the undetectable levels of virus-neutralizing antibody, may be attributable to the magnitude of antigenic differences between VN and rgAnhui viruses, as HI titers of VN virus were 64-fold lower when compared to the homologous titer of anti-rgAnhui ferret antiserum, and the VN virus apparently differed greatly in antigenicity when compared with the rgAnhui vaccine virus (Table 1). The results indicate that, for the rgAnhui vaccine, enhanced immunogenicity due to addition of adjuvant and/or increasing the antigen dose is necessary to neutralize clade 1 viruses.

The rgAnhui vaccine induced intermediate levels of cross-reactive neutralizing antibody against clade 2.2 Tk virus (Fig. 1), and only a low dose of non-adjuvanted vaccine showed reduced cross-protection (60%) to challenge infection with Tk virus (Fig. 4C). This result was also correlated with the magnitude of antigenic difference between Tk virus and rgAnhui virus, as the HI titer of Tk virus was 16-fold lower when compared with the homologous titer (Table 1). The survival rate of control mice challenged with Tk virus was 40%, in contrast to the 0% seen with other viruses, despite inoculation with the $20 \times MLD_{50}$ dose calculated by the Reed and Muench method. However, 1–2 of the 5 control mice challenged with $20 \times MLD_{50}$, or higher doses, of Tk virus survived in several independent experiments (data not shown). As all control mice challenged with Tk virus showed unrecoverable weight loss (Fig. 5C) and virus-neutralizing antibody titers in the sera of surviving control mice on day 14 after challenge were comparable to those of vaccinated mice (data not shown), the higher survival rate in control mice was not due to a technical failure, but was attributable to the features of the TK virus itself.

Addition of adjuvant improved the protection efficacy against TK virus, but the severity of weight loss in vaccinated mice was markedly higher than with clade 1 VN virus (Fig. 5A and C), despite intermediate levels of neutralizing antibodies being elicited by rgAnhui vaccine. The MLD_{50} values for VN and Tk viruses were 5.1×10^2 $TCID_{50}$ and 2.3×10^6 $TCID_{50}$, respectively. Consequently, the input amount of Tk virus for lethal infection was 4510-times greater when compared to VN virus. This difference may have been reflected in the severity of weight loss.

Despite undetectable levels of virus-neutralizing antibody after non-adjuvanted vaccine, all mice infected with Myan and Indo viruses and 20–80% mice infected with VN virus, respectively, survived (Figs. 1, 2 and 4). Nonetheless, high levels of HA-specific IgG1 and IgG2a antibodies against these viruses were elicited (Figs. 6 and 7), but it is unlikely that non-neutralizing HA-specific antibodies contributed to the survival of virus-infected mice, as HA-specific IgG1 and IgG2a antibodies were also induced in the sera of mice vaccinated but did not survived from following lethal virus challenge. Consequently, the method of virus-neutralizing assay may be less sensitive for evaluating mouse survival after lethal challenge infection.

In the present study, the efficacy of H5N1 vaccine derived from clade 2.3.4, rgAnhui, was assessed based on broad immunogenicity and cross-protection by challenge infection. The rgAnhui vaccine was shown in a mouse model to produce broad-spectrum immunity and to protect against not only homologous infections, but also heterologous clade H5N1 HPAIVs, when the vaccine was conjugated with alum to enhance immunogenicity. Human infections with H5N1 HPAIVs have been continuously reported since 2003, and the antigenic features of the isolates from humans, poultry and wild birds have became variable among the HA genetic clades [34]. Although several H5N1 vaccine candidate viruses chosen from 8 clades (1, 2.1, 2.2, 2,2.1, 2.3.2, 2.3.4, 4 and 7) have been developed and updated [24], it is impossible to prepare stockpile vaccines using all recently available vaccine candidates. The rgAnhui vaccine virus possesses broad cross-immunity, and is therefore a promising candidate for the production of stockpile H5N1 vaccine. In fact, rgAnhui virus was selected for the Japanese national stockpile vaccine in 2007 [35].

Acknowledgements

We would like to thank Dr. Phengta Vongprachanh, National Center for Laboratory and Epidemiology, Lao PDR, Dr. Khin Yi Oo, National Health Laboratory, Myanmar, and Dr. L.T.Q. Mai, National Institute of Health and Epidemiology, Viet Nam, for providing clinical specimens for isolation of A/Laos/JP127/2009, A/Myanmar/JPA007-07/2007 and A/VietNam/JP1203/2004, respectively. We are also grateful to Dr. Nancy Cox, US-CDC, Dr. Alan Hay, National Institute of Medical Research, and Dr. Malik Peiris, University of Hong Kong, for providing rgAnhui01/2005 vaccine virus and post-infection ferret sera, A/Turkey/12/2006, A/Indonesia/5/2005 and A/Japanese White Eye/HK/1038/2005, respectively. These studies were supported by a Health Labor Sciences Research Grant from the Ministry of Health, Labor and Welfare of Japan and by the Program for Promotion of Fundamental Studies in Health Sciences of the National Institute of Biomedical Innovation (NIBIO).

References

[1] Claas EC, Osterhaus AD, van Beek R, De Jong JC, Rimmelzwaan GF, Senne DA, et al. Human influenza A H5N1 virus related to a highly pathogenic avian influenza virus. Lancet 1998;351(February (9101)):472–7.
[2] Subbarao K, Klimov A, Katz J, Regnery H, Lim W, Hall H, et al. Characterization of an avian influenza A (H5N1) virus isolated from a child with a fatal respiratory illness. Science 1998;279(January (5349)):393–6.
[3] World Health Organization. Cumulative number of confirmed human cases of avian influenza A/(H5N1) reported to WHO; 2011, cited. Available from: http://www.who.int/csr/disease/avian_influenza/country/cases_table_2011_08_02/en/index.html.
[4] Normile D. Avian influenza human transmission but no pandemic in Indonesia. Science 2006;312(June (5782)):1855.

[5] Tran TH, Nguyen TL, Nguyen TD, Luong TS, Pham PM, Nguyen VC, et al. Avian influenza A (H5N1) in 10 patients in Vietnam. N Engl J Med 2004;350(March (12)):1179–88.
[6] Ungchusak K, Auewarakul P, Dowell SF, Kitphati R, Auwanit W, Puthavathana P, et al. Probable person-to-person transmission of avian influenza A (H5N1). N Engl J Med 2005;352(January (4)):333–40.
[7] Ministry of Agriculture FaFoJ; 2011, cited; Available from: http://www.maff.go.jp/j/syouan/douei/tori/pdf/110405_ai_japan_map.pdf.
[8] Ministry of Health LaW; 2004, cited; Available from: http://www.mhlw.go.jp/topics/bukyoku/kenkou/tori/041222/1.html.
[9] Nicolson C, Major D, Wood JM, Robertson JS. Generation of influenza vaccine viruses on Vero cells by reverse genetics: an H5N1 candidate vaccine strain produced under a quality system. Vaccine 2005;23(April (22)):2943–52.
[10] Dong J, Matsuoka Y, Maines TR, Swayne DE, O'Neill E, Davis CT, et al. Development of a new candidate H5N1 avian influenza virus for pre-pandemic vaccine production. Influenza Other Respi Viruses 2009;3(November (6)):287–95.
[11] Webby RJ, Perez DR, Coleman JS, Guan Y, Knight JH, Govorkova EA, et al. Responsiveness to a pandemic alert: use of reverse genetics for rapid development of influenza vaccines. Lancet 2004;363(April (9415)):1099–103.
[12] Treanor JJ, Campbell JD, Zangwill KM, Rowe T, Wolff M. Safety and immunogenicity of an inactivated subvirion influenza A (H5N1) vaccine. N Engl J Med 2006;354(March (13)):1343–51.
[13] Ninomiya A, Imai M, Tashiro M, Odagiri T. Inactivated influenza H5N1 whole-virus vaccine with aluminum adjuvant induces homologous and heterologous protective immunities against lethal challenge with highly pathogenic H5N1 avian influenza viruses in a mouse model. Vaccine 2007;25(May (18)):3554–60.
[14] Brady RC, Treanor JJ, Atmar RL, Keitel WA, Edelman R, Chen WH, et al. Safety and immunogenicity of a subvirion inactivated influenza A/H5N1 vaccine with or without aluminum hydroxide among healthy elderly adults. Vaccine 2009;27(August (37)):5091–5.
[15] Lin J, Zhang J, Dong X, Fang H, Chen J, Su N, et al. Safety and immunogenicity of an inactivated adjuvanted whole-virion influenza A (H5N1) vaccine: a phase I randomised controlled trial. Lancet 2006;368(September (9540)):991–7.
[16] Naim JO, van Oss CJ, Wu W, Giese RF, Nickerson PA. Mechanisms of adjuvancy: I—metal oxides as adjuvants. Vaccine 1997;15(August (11)):1183–93.
[17] Bernstein DI, Edwards KM, Dekker CL, Belshe R, Talbot HK, Graham IL, et al. Effects of adjuvants on the safety and immunogenicity of an avian influenza H5N1 vaccine in adults. J Infect Dis 2008;197(March (5)):667–75.
[18] Leroux-Roels G. Prepandemic H5N1 influenza vaccine adjuvanted with AS03: a review of the pre-clinical and clinical data. Expert Opin Biol Ther 2009;9(August (8)):1057–71.
[19] Europian Medicines Agency. Aflunov, cited; Available from: http://www.ema.europa.eu/ema/index.jsp?curl=pages/medicines/human/medicines/002094/human_med_001396.jsp&murl=menus/medicines/medicines.jsp&mid=WC0b01ac058001d125.
[20] Europian Medicines Agency. Prepandemic influenza vaccine (H5N1) Novartis Vaccines and Diagnostic, cited; Available from: http://www.ema.europa.eu/ema/index.jsp?curl=pages/medicines/human/medicines/002269/human_med_001397.jsp&murl=menus/medicines/medicines.jsp&mid=WC0b01ac058001d125.
[21] Europian Medicines Agency. Prepandrix, cited; Available from: http://www.ema.europa.eu/ema/index.jsp?curl=pages/medicines/human/medicines/000822/human_med_000986.jsp&murl=menus/medicines/medicines.jsp&mid=WC0b01ac058001d125.
[22] Europian Medicines Agency. Pandemic influenza vaccine (H5N1) (split virion, inactivated, adjuvanted) GlaxoSmithKline Biologicals, cited; Available from: http://www.ema.europa.eu/ema/index.jsp?curl=pages/medicines/human/medicines/001206/human_med_001214.jsp&murl=menus/medicines/medicines.jsp&mid=WC0b01ac058001d125.
[23] World Health Organization. Antigenic and genetic characteristics of H5N1 viruses and candidate H5N1 vaccine viruses developed for potential use as pre-pandemic vaccines; 2005, cited; Available from: http://www.who.int/csr/disease/avian_influenza/guidelines/recommendationvaccine.pdf.
[24] World Health Organization. Antigenic and genetic characteristics of influenza A (H5N1) and influenza A(H9N2) viruses and candidate vaccine viruses developed for potential use in human vaccines; 2011, cited; Available from: http://www.who.int/csr/disease/avian_influenza/guidelines/2011_02_h5_h9_vaccinevirusupdate.pdf.
[25] Takahashi Y, Hasegawa H, Hara Y, Ato M, Ninomiya A, Takagi H, et al. Protective immunity afforded by inactivated H5N1 (NIBRG-14) vaccine requires antibodies against both hemagglutinin and neuraminidase in mice. J Infect Dis 2009;199(June (11)):1629–37.
[26] Brewer JM, Conacher M, Hunter CA, Mohrs M, Brombacher F, Alexander J. Aluminium hydroxide adjuvant initiates strong antigen-specific Th2 responses in the absence of IL-4- or IL-13-mediated signaling. J Immunol 1999;163(December (12)):6448–54.
[27] Brewer JM, Conacher M, Satoskar A, Bluethmann H, Alexander J. In interleukin-4-deficient mice, alum not only generates T helper 1 responses equivalent to freund's complete adjuvant, but continues to induce T helper 2 cytokine production. Eur J Immunol 1996;26(September (9)):2062–6.
[28] Fazekas G, Rosenwirth B, Dukor P, Gergely J, Rajnavolgyi E. IgG isotype distribution of local and systemic immune responses induced by influenza virus infection. Eur J Immunol 1994;24(December (12)):3063–7.
[29] Palladino G, Mozdzanowska K, Washko G, Gerhard W. Virus-neutralizing antibodies of immunoglobulin G (IgG) but not of IgM or IgA isotypes can cure influenza virus pneumonia in SCID mice. J Virol 1995;69(April (4)):2075–81.
[30] Bomford R. The comparative selectivity of adjuvants for humoral and cell-mediated immunity. II. Effect on delayed-type hypersensitivity in the mouse and guinea pig, and cell-mediated immunity to tumour antigens in the mouse of Freund's incomplete and complete adjuvants, alhydrogel, Corynebacterium parvum, Bordetella pertussis, muramyl dipeptide and saponin. Clin Exp Immunol 1980;39(February (2)):435–41.
[31] Reiss CS, Schulman JL. Cellular immune responses of mice to influenza virus vaccines. J Immunol 1980;125(November (5)):2182–8.
[32] Wijburg OL, van den Dobbelsteen GP, Vadolas J, Sanders A, Strugnell RA, van Rooijen N. The role of macrophages in the induction and regulation of immunity elicited by exogenous antigens. Eur J Immunol 1998;28(February (2)):479–87.
[33] Lu X, Edwards LE, Desheva JA, Nguyen DC, Rekstin A, Stephenson I, et al. Cross-protective immunity in mice induced by live-attenuated or inactivated vaccines against highly pathogenic influenza A (H5N1) viruses. Vaccine 2006;24(November (44–46)):6588–93.
[34] World Health Organization. Weekly epidemiological record; 2011, cited; Available from: http://www.who.int/wer/2011/wer8617.pdf.
[35] Ministry of Health LaW. Annual health, labour and welfare report 2007–2008; 2008, cited; Available from: http://www.mhlw.go.jp/english/wp/wp-hw2//part2//p2c1s7a.pdf.

International Immunology, Vol. 23, No. 7, pp. 433–441
doi:10.1093/intimm/dxr031
Advance Access publication 3 June 2011

HIV-1 Nef impairs multiple T-cell functions in antigen-specific immune response in mice

Hideki Fujii[1,2,*], Manabu Ato[2,*], Yoshimasa Takahashi[2], Kaori Otake[3], Shu-ichi Hashimoto[4], Tomohiro Kaji[5], Yasuko Tsunetsugu-Yokota[2], Mikako Fujita[6], Akio Adachi[7], Toshinori Nakayama[8], Masaru Taniguchi[9], Shigeo Koyasu[1] and **Toshitada Takemori[2,5]**

[1]Department of Microbiology and Immunology, Keio University School of, Medicine, Tokyo 160-8582, Japan
[2]Department of Immunology, National Institute of Infectious Diseases, Tokyo 162-8640, Japan
[3]Gifu Social Insurance Hospital, Gifu 509-0206, Japan
[4]Chiome Bioscience Inc., Saitama 351-0104, Japan
[5]Laboratory for Immunological Memory, Riken Research Center for Allergy and Immunology, Kanagawa 230-0045, Japan
[6]Department of Bioorganic Medicinal Chemistry, Faculty of Medical and Pharmaceutical Sciences, Kumamoto University, Kumamoto 862-0973, Japan
[7]Department of Virology, Institute of Health Biosciences, The University of Tokushima Graduate School, Tokushima 770-8503, Japan
[8]Department of Immunology, Graduate School of Medicine, Chiba University, Chiba 260-8670, Japan
[9]Laboratory for Immune Regulation, Riken Research Center for Allergy and Immunology, Kanagawa 230-0045, Japan

*These authors contributed equally to this study.

Correspondence to: T. Takemori; E-mail: mttoshi@rcai.riken.jp

Received 10 February 2011, *accepted* 2 May 2011

Abstract

The viral protein Nef is a key element for the progression of HIV disease. Previous *in vitro* studies suggested that Nef expression in T-cell lines enhanced TCR signaling pathways upon stimulation with TCR cross-linking, leading to the proposal that Nef lowers the threshold of T-cell activation, thus increasing susceptibility to viral replication in immune response. Likewise, the *in vivo* effects of Nef transgenic mouse models supported T-cell hyperresponse by Nef. However, the interpretation is complicated by Nef expression early in the development of T cells in these animal models. Here, we analyzed the consequence of Nef expression in ovalbumin-specific/CD4$^+$ peripheral T cells by using a novel mouse model and demonstrate that Nef inhibits antigen-specific T-cell proliferation and multiple functions required for immune response *in vivo*, which includes T-cell helper activity for the primary and memory B-cell response. However, Nef does not completely abrogate T-cell activity, as defined by low levels of cytokine production, which may afford the virus a replicative advantage. These results support a model, in which Nef expression does not cause T-cell hyperresponse in immune reaction, but instead reduces the T-cell activity, that may contribute to a low level of virus spread without viral cytopathic effects.

Keywords: AIDS, acquired immunity, humoral response

Introduction

The Nef protein of the primate lentiviruses HIV-1/2 and the simian immunodeficiency virus (SIV) is expressed from the earliest stage of viral gene expression (reviewed in ref. 1). Nef-defective viruses cause a slow progression of clinical disease with reduced viral loads in humans and rhesus macaques with HIV-1/2 and SIV infection, respectively, indicating that Nef plays a crucial role in viral pathogenesis in human and non-human primates (reviewed in ref. 1). Nef associates with host cell membranes through N-terminal myristoylation and functions as an adaptor bringing together a large number of proteins in host cells, mainly protein kinases and components of endocytic trafficking machinery (reviewed in ref. 1; refs 2–7).

Nef reduces surface level receptors, including CD4, the primary receptor for HIV and SIV and MHC class I and class II complex, facilitating HIV immune evasion and thus increases viral pathogenesis (reviewed in ref. 1). Additionally, extensive *in vitro* studies, mostly carried out by using human T-cell lines, have suggested that Nef expression enhances TCR-mediated signaling pathways and transcriptional activation (reviewed in ref. 1; refs 2–5). Such alterations in signaling events may lower the TCR activation threshold in CD4$^+$

T cells and help more responsive to T-cell activation signals, a process that could support higher virus production upon stimuli mediated via the TCR (reviewed in ref. 1; refs 2–5). Moreover, Nef may alter host cell death pathways to prevent apoptosis of infected cells, thereby fostering their longevity (reviewed in ref. 1) These observations have led to a model in which Nef reorganizes the host cell activity so as to optimize viral propagation and cell survival, thus facilitating immune evasion and participating in virus spread.

The consequence of Nef expression in primary cells has been examined by using Nef transgenic (Tg) mice, in which Nef was constitutively or transiently expressed under control of a T-cell-specific promoter–enhancer element (8, 9). In this model system, Nef promotes T-cell activation, however, interpretation of these findings is complicated by the fact that expression of Nef early in the development of T cells results in wholesale depletion of thymocytes and peripheral T cells. Moreover, it remains obscure whether the T-cell activation seen in Nef Tg mice is mediated by lymphopenia-induced mechanisms rather than by an intrinsic effect of Nef expression on T-cell activation and proliferation (9, 10).

In the present study, to examine the consequence of Nef expression in primary cells, we established a double transgenic mouse (dTg), which expresses human coxsackie/adenovirus receptor (CAR) (11) and an ovalbumin (OVA)-specific TCR that recognizes the OVA peptide on antigen-presenting cell (APC) with high affinity under MHC Class II I-A^d-restriction. This system allowed us to analyze the effect of Nef on antigen-specific peripheral T-cell function by transfer of the *nef* gene into peripheral T cells using an adenovirus vector. The present study demonstrates that Nef expression does not cause T-cell hyperresponse but instead impairs T-cell functions required for immune response.

Methods

Mice

BALB/c and CB17-scid mice were purchased from Shizuoka Laboratory Animal Center (Hamamatsu, Japan) and Clea Japan, Inc. (Tokyo, Japan), respectively. Tg mice expressing the CAR under the control of the Lck proximal promoter (CAR Tg mice) on the BALB/c background have been described previously (11). DO11.10 mice express a transgenic TCR with specificity for OVA peptide residues 323–339 ($OVA_{323-339}$) restricted by I-A^d on the BALB/c background (12). All mice used in this study were maintained under specific pathogen-free conditions and used at 6–12 weeks of age in accordance with the guidelines of the Institutional Animal Care and Use Committee, National Institute of Infectious Diseases.

Adenovirus vector

Recombinant adenovirus vectors were generated using the AdEasy Adenoviral Vector System (Stratagene) according to the manufacturer's instructions. In order to express the *nef* gene under the CAG promoter, the pShuttle vector was digested with *Kpn*I, blunt-ended with T4 polymerase and then, the CAG promoter DNA was ligated (pShuttle-CAG). Next, an *Xho*I–*Xba*I fragment of pIRES2-EGFP (Invitrogen) was inserted into the *Xho*I–*Xba*I site of pShuttle-CAG, which was designated as pShuttle-CAG-I2-EGFP. HIV-1 NL4-3 nef wild-type and a mutant ($^{57}W^{58}L$ to $^{57}A^{58}A$) were PCR amplified from pNL432 and pNL-n57/2A proviral DNA, respectively, using specific primers containing *Eco*RI sites at both ends and then subcloned into pBluscript KS^+ (Stratagene). The *Eco*RI fragment containing wild-type or mutant nef was inserted into the *Eco*RI site of pShuttle-CAG-I2-EGFP. These shuttle vectors were linearized and co-transformed into *Escherichia coli* strain BJ5183-AD-1, which contains the pAdEasy vector, to induce homologous recombination (Supplementary Figure 1 is available at *International Immunology* Online). Recombinant adenoviral plasmids were selected and transfected into 293 cells to produce recombinant adenovirus particles. Recombinant adenovirus were purified by two rounds of Cesium chloride density gradient centrifugation as described previously (13). The concentrated virus was dialyzed against PBS containing 10% glycerol. The titer of the virus stock was determined by a plaque formation assay using 293 cells.

T-cell purification and recombinant adenovirus infection

For recombinant adenovirus infection, $CD4^+$ T cells were enriched by negative selection on a MACS column (Miltenyi Biotec GmbH, Gladbach, Germany) as previously described (14). Briefly, cells were blocked with anti-FcγRII/III (2.4G2; BD PharMingen, San Diego, CA, USA) and incubated with biotinylated mAbs against B220(RA3-6B2), IgM(II/41), IgD(11-26), Gr1(RB6-8C5), CD11c(N418), CD49b(DX5), CD11b(M1/70) and CD8(53–6.7) (eBioscience, San Diego, CA, USA), followed by incubation with streptavidin-coated microbeads (Miltenyi Biotec GmbH). Purified $CD4^+$ T cells (>95%) were infected with recombinant adenovirus vector at a multiplicity of infection of 10 (MOI 10) for 2 days in 24-well plates at a concentration of 2×10^6 per well in RPMI 1640 medium supplemented with 10% Fetal Bovine Serum (FBS), 5×10^5 M 2-mercaptoethanol, L-glutamine, antibiotics and IL-7 (20 ng ml^{-1}; PeproTech, London, UK) at 37°C in an atmosphere of 5% CO_2.

Proliferation assays and ELISA

Sorted $CD4^+$ GFP^+ T cells were cultured in microtiter wells at a concentration of 4×10^4 cells per well in the presence of $OVA_{323-339}$ peptide and 5×10^5 irradiated T-depleted spleen cells. DNA synthesis of cultured cells in triplicate was estimated by the incorporation of [^{3}H] thymidine (0.5 μCi) added 12 h prior to cell harvest. The level of IFN-γ and IL-2 in the culture supernatants was measured by a Ready-Set-Go! ELISA assay kit (eBioscience), according to the manufacturer's instruction. In some experiments, $CD4^+$ GFP^+ T cells (2×10^6) were cultured for 2–3 days in 96-well plates immobilized with anti-TCR mAb (5 μg ml^{-1}) and anti-CD28 mAb (1 μg ml^{-1}) (BD PharMingen).

Chemotaxis assay

Chemotaxis assays were performed in Transwell (Corning Coster, Coring, NY, USA) with polycarbonate filters (5 μm pore size) as described previously (15). Briefly, purified $CD4^+$ GFP^+ T cells were suspended at 5×10^6 cells ml^{-1} in RPMI 1640 medium containing 1% FBS and 25 mM HEPES. One

hundred microliters of cell suspension was loaded onto the upper wells and placed in a 24-well plate containing 600 μl of media with the indicated doses of CXCL12 (SDF-1α) (PeproTech) or CCL19 (ELC) (R&D Systems, Minneapolis, MN, USA). Cells were incubated at 37°C for 90 min, and cells in the bottom wells were counted using a FACSCalibur.

Activation-induced cell death assay

Sorted $CD4^+$ GFP^+ T cells were cultured at a concentration of 1×10^6 cells ml^{-1} in 96-well plates immobilized with 5 μg ml^{-1} of anti-CD3ε mAb (2C11) (BioLegend, San Diego, CA, USA) in RPMI medium supplemented with 10% FBS. Cells were harvested 2 days later and then re-cultured for 3 days in 96-well plates containing immobilized with anti-CD3 mAb or medium containing 200 U ml^{-1} of human IL-2 (PeproTech). To detect apoptotic cells, a terminal deoxynucleotidyl transferase-mediated deoxyuridine triphosphate nick end labeling assay was performed using the ApopTag Red In Situ Apoptosis Detection Kit (CHEMICON International Inc., Temecula, CA, USA). Briefly, the cells were collected and deposited on glass slides by cytospin (Shandon, London, UK), fixed with PBS containing 1% PFA for 10 min and the DNA free 3′ OH were enzymatically labeled with digoxigenin-labeled nucleotides, which were detected using rhodamine-labeled anti-digoxigenin polyclonal antibodies according to the manufacturer's instructions. After applying 6 μg ml^{-1} of Hoechst33342 (Invitrogen) for nuclear staining, slides were processed for analysis using an LSM 510 laser-scanning confocal microscope (Carl Zeiss, Jena, Germany). The proportion of apoptotic cells was determined by counting at least 100 cells in the captured images.

T-cell migration in vivo

BALB/c mice were intravenously injected with 2×10^6 of purified $CD4^+$ GFP^+ T cells uninfected or infected with a recombinant adenovirus vector. Twenty-four hours later, the recipient mice were subcutaneously immunized with 0.2 mg of LPS-free OVA in CFA on the back at three sites. The number of $CD4^+KJ1\text{-}26^+$ T cells in the draining lymph nodes was measured by flow cytometry at 5 days after immunization.

Adoptive cell transfer

Transfer of B cells and OVA-specific/$CD4^+$ T cells infected with a recombinant adenovirus vector in adoptive hosts was performed as described previously (14).

Briefly, $CD4^+$ GFP^+ T cells were prepared by FACS sorting from dTg T cells infected with a recombinant adenovirus vector *in vitro*. B cells were negatively selected from the pooled spleens of either naive mice or 4-hydroxyl-3-nitrophenylacetyl-conjugated chicken γ-globulin (NP-CGG)-primed mice using a MACS system and biotinylated anti-CD5 (53–7.3), anti-CD90.2 (53–2.1), anti-Gr1, anti-CD11b (eBioscience), anti-CD43 (57) and anti-CD138 (281-2) (BD PharMingen). The procedure consistently yielded >95% $B220^+$ cells. Purified B cells (5×10^6) together with $CD4^+$ GFP^+ T cells infected with recombinant adenovirus vector (3×10^4) were intravenously injected into CB17-scid mice. One day later, the recipient mice were intraperitoneally challenged with 25 μg of soluble NP-OVA, and the sera were collected from individual mice at day 7 after challenge. Anti-NP serum antibody titers were estimated by ELISA assays using NP_2-BSA and NP_{18}-BSA as coating antigens as described previously (14). The relative affinity of anti-NP antibodies was estimated by calculating the ratio of anti-NP_2/anti-NP_{18} antibody.

Statistics

The results were evaluated statistically by two-tailed Student's *t*-test ($n = 3$) or Mann–Whitney nonparametric test ($n > 4$), with $P < 0.05$ regarded as significant.

Results

Nef impairs T-cell proliferation upon antigen stimulation in vitro

In order to determine the effect of Nef expression in peripheral T cells, we crossed Tg mice that express an OVA-specific T-cell receptor (12) with mice expressing CAR on T cells (11). OVA-specific/$CD4^+$/CAR^+ T cells were purified from the pooled spleens of dTg mice and infected *in vitro* with an adenovirus vector encoding green fluorescence protein (GFP) driven by the CAG promoter with (Ad-nef) or its mutants [Ad-nef (mu)] or without the *nef* gene (Ad) in the presence of IL-7, which supports T-cell survival and promotes progression into the G_{1b} stage of the cell cycle (16, 17). Thereafter, GFP^+ cells were purified by FACS and provided for analysis as below.

Consistent with previous observations in human T-cell lines, Fig. 1(A) shows that CD4 expression on murine peripheral T cells was down-regulated by Nef but not by the Nef mutant carrying amino acids replacements of $^{57}W^{58}L$ to $^{57}A^{58}A$, abrogating the ability to down-regulate CD4 (18). Nef expression had no effect on the expression of CD25, CD28, CD44, CD62L, CD69, TCRβ and MHC class I (data not shown).

To examine the effect of Nef in T-cell response, GFP^+ cells were purified by FACS from $CD4^+$/CAR^+ T cells infected with Ad-nef, Ad-nef (mu) and cultured in the presence of irradiated splenocytes as APCs, which had been pulsed with OVA peptide ($OVA_{323–339}$). Expression of wild-type as well as mutant forms of Nef diminished T-cell proliferation upon stimulations with OVA peptide at a dose of 0.1 μM (Fig. 1B). These Nef proteins also reduced the level of cytokines produced by T cells in response to different doses of OVA peptide (Fig. 1C). These results suggest that Nef prominently affects T-cell proliferation, irrespective of Nef's ability to down-modulate CD4 but not completely abrogate T-cell activation.

Nef-expression diminishes T-cell migration activity in the primary immune response

Chemokines and their receptors play pivotal roles in the initial homing of lymphocytes and their subsequent trafficking during an immune response (6). It has been reported that Nef impairs the migratory capacity of human T-cell lines *in vitro* in response to the chemokine CXCL12, which binds to T-cell receptor, CXCR4, owing to alteration of the signal cascades downstream of chemokine receptors (7, 15). Consistently, the expression of Nef or its mutant in murine $CD4^+$ T cells reduced their migration in response to CXCL12 *in vitro*, without altering the surface receptor expressions (Fig. 2A and B).

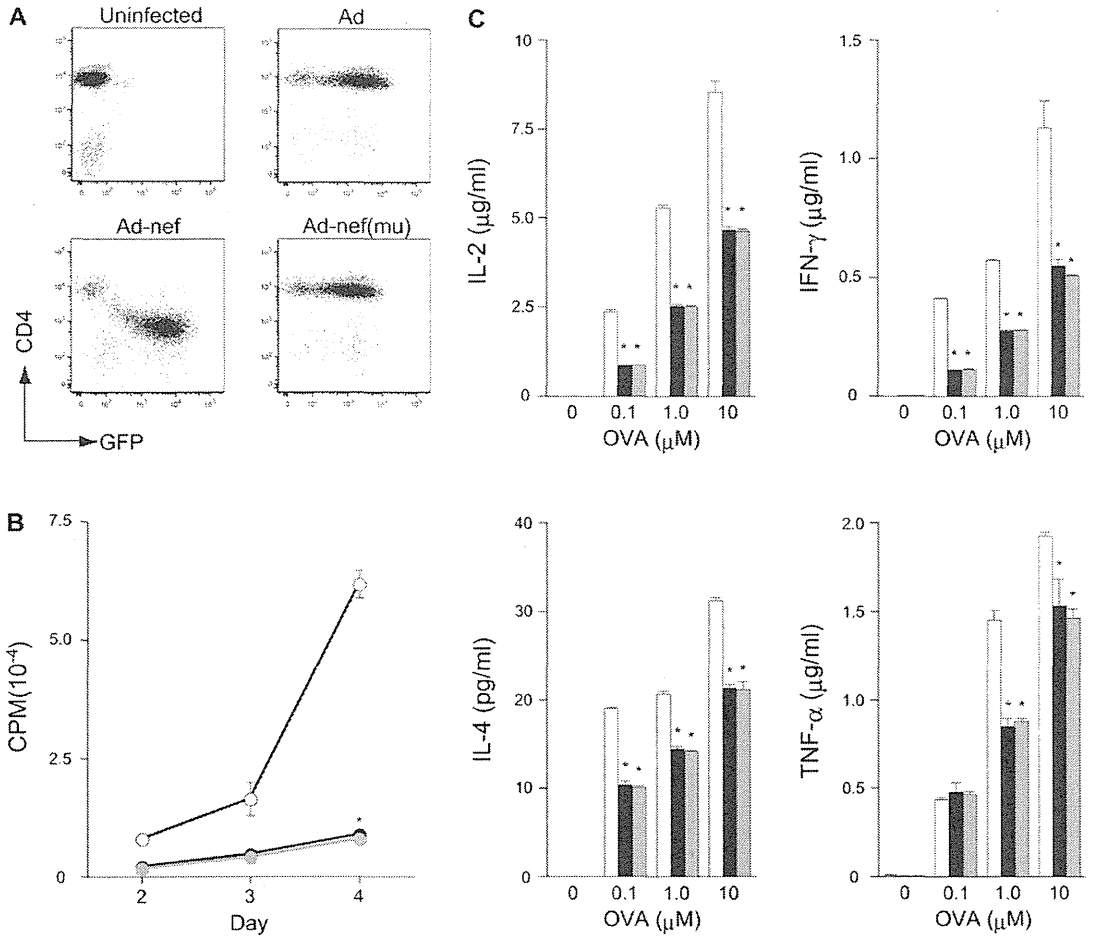

Fig. 1. (A) Characterization of Nef-expressing T cells. A *EGFP* gene-containing adenoviral vector was used to evaluate the efficiency of adenovirus (Ad) infection in DO11.10/CAR$^+$/CD4$^+$ T cells. Naive CD4$^+$ T cells from dTg mice were infected with Ad-nef, Ad-nef (mu) or Ad vector as a control. Two days later, GFP and CD4 expression were assessed by FACS. (B) Nef represses antigen-specific T-cell proliferation. Purified CD4$^+$/GFP$^+$ T cells (5×10^4) infected with Ad-nef (closed), Ad-nef (mu) (gray) and Ad (open) were cultured with T-cell depleted spleen cells as APCs (5×10^5) pulsed with 0.1 μM of $OVA_{323-339}$ peptide. Their DNA synthesis in the triplicate culture was estimated at the indicated periods by the incorporation of [^{3}H] thymidine added 12 h prior to cell harvest. *$P < 0.001$ versus Ad. (C) Purified CD4$^+$ GFP$^+$ T cells and APCs were co-cultured with various concentrations of $OVA_{323-339}$ peptide. Cytokine production in culture supernatant was measured by ELISA on day 3 of culture. *$P < 0.001$ versus Ad. Shown is the representative data from two independent experiments.

Likewise, the Nef proteins, including NL4-3 Nef, did not alter the expression of CXCR4 on human T cells (15, 19), however, there are controversial reports that HIV-1 Nef caused a modest decrease in expression of CXCR4 on human T cells, irrespective of Nef alleles, including NA7 and NL4-3 (7, 20). Further analysis is needed to resolve the discrepancy among these studies.

To examine whether Nef affects T-cell migration *in vivo*, OVA-specific CD4$^+$ T cells were purified from pooled splenocytes of dTg mice and infected with Ad-nef, Ad-nef(mu) or Ad. These cells were transferred into syngeneic recipients, followed by subcutaneous inoculation with OVA in CFA. Five days later, the frequency of OVA-specific (KJ1-26$^+$) CD4$^+$ T cells in the draining lymph node was estimated by FACS. As shown in Fig. 2(C), we observed that Nef impairs the physiological recruitment of T cells into the secondary lymphoid tissues in the immune response. A substantial number of GFP$^+$/OVA-specific/CD4$^+$ T cells infected with Ad accumulated in the draining lymph node after OVA stimulation, however, the number of cells was significantly reduced when the T cells expressed Nef or its mutant. T cells in the draining lymph nodes uniformly expressed high levels of CD44, a marker for activated T cells (21), irrespective of their expression of Nef or Nef mutant (Fig. 2D), suggesting that they were activated, but not involved in functional maturation. These results suggest that Nef affects trafficking of T cells to the regional lymph nodes during an immune response, independently of CD4 down-modulation.

As shown in Fig. 2(E), we examined the possibility that nef expression causes T cells to undergo AICD, which could reduce the number of cells migrating to the regional lymph nodes after stimulation. OVA-specific/CD4$^+$ or

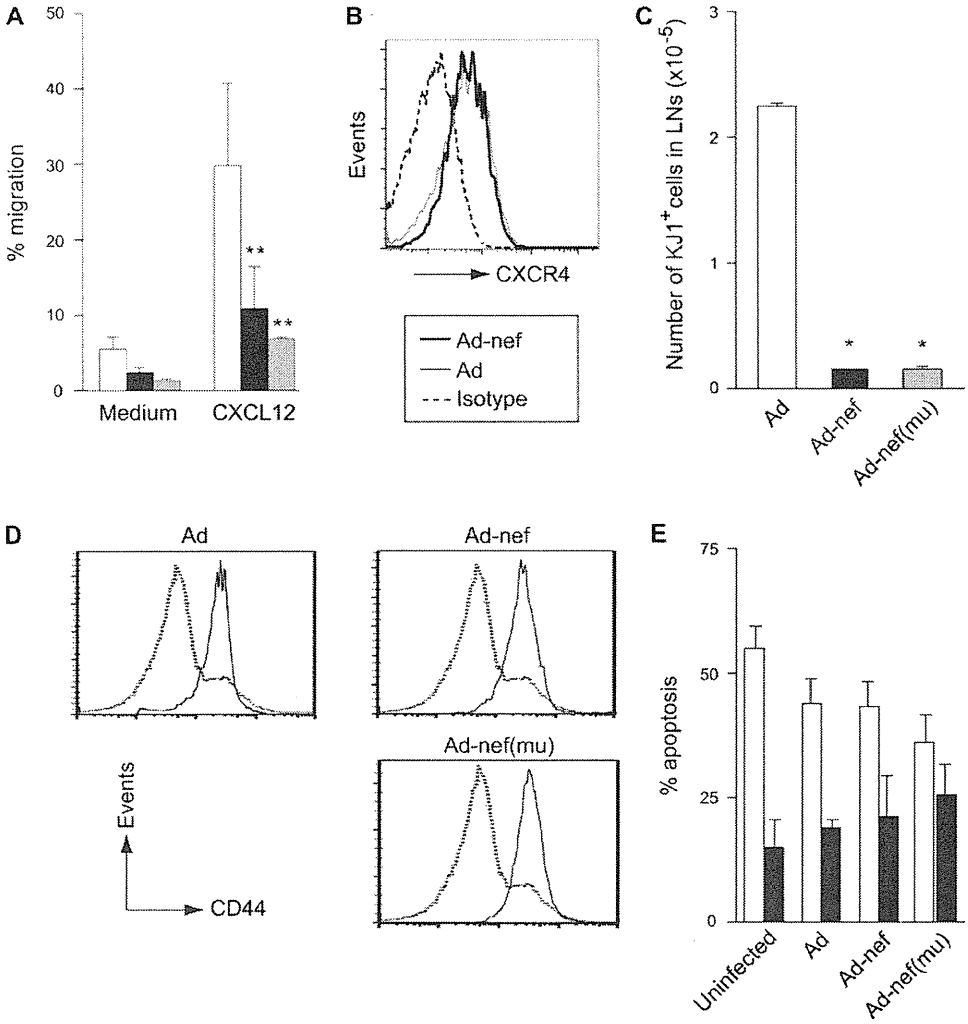

Fig. 2. Nef impairs T-cell migratory activity (A). $CD4^+$ GFP^+ T cells infected with Ad-nef (closed column), Ad-nef (mu) (gray column) and Ad (open column) were used in transwell chemotaxis assays in the presence of CXCL12 (PeproTech). Cells were allowed to migrate in the bottom wells for 90 min, and the proportion of cells that had migrated into the lower wells was determined by flow cytometry. The results are shown as mean ± SD ($n = 3$). $^*P < 0.01$ versus Ad. (B) CXCR4 surface staining for $CD4^+/GFP^+$ T cells after infection with Ad-nef (solid line) or Ad (thin line), together with control IgG staining (broken lines). (C and D) $CD4^+/GFP^+$ T cells (2×10^6) infected with Ad-nef (closed column), Ad-nef (mu) (gray column) and Ad (open column) were transferred into BALB/c mice and 24 h later mice were injected subcutaneously with 0.2 mg of LPS-free OVA with CFA on the back in three sites. The cell number (±SD) of $CD4^+$/OVA-specific T cells in the draining lymph nodes (C) and the level of CD44 expression in Ad-infected donor (solid line) and recipient $CD4^+$ T cells (broken line) (D) were measured by flow cytometry using anti-CD4, anti-CD44 and KJ1-26 mAbs on day 5 after OVA injection. $^*P < 0.001$ versus Ad. (E) $CD4^+$ T cells (1×10^6) or $CD4^+/GFP^+$ T cells (1×10^6) infected with Ad-nef, Ad-nef (mu) and Ad were stimulated with immobilized anti-CD3ε mAb for 2 days, followed by re-stimulation with anti-CD3 mAb/IL-2 (open column) or IL-2 alone (closed column) for 3 days. Apoptotic cells were analyzed by terminal deoxynucleotidyl transferase-mediated deoxyuridine triphosphate nick end labeling assay. Representative data from two independent experiments in (A), (C) and (D) and from three independent experiments (B) is shown.

OVA-specific/$CD4^+/GFP^+$ T cells were hyperstimulated with immobilized anti-CD3ε mAb at 2-day intervals as previously described (22). The results show that Nef did not enhance the induction of AICD in T cells upon TCR-stimulation *in vitro* nor did it compromise the survival function mediated by IL-2. Therefore, it seems unlikely that Nef causes T-cell death, which could reduce the number of cells migrating to the regional lymph nodes.

Nef expression in T cells affects the primary and memory B-cell responses

To examine T-cell helper activity by Nef, OVA-specific/$CD4^+$ T cells were purified from the pooled spleens of dTg mice, followed by infection with or without Ad-nef, Ad-Nef (mu) or Ad. The $GFP^+/CD4^+$ T cells were purified by FACS (Fig. 3A) and transferred into CB17-scid mice, together with either naive or NP-primed B cells. The recipients were immunized

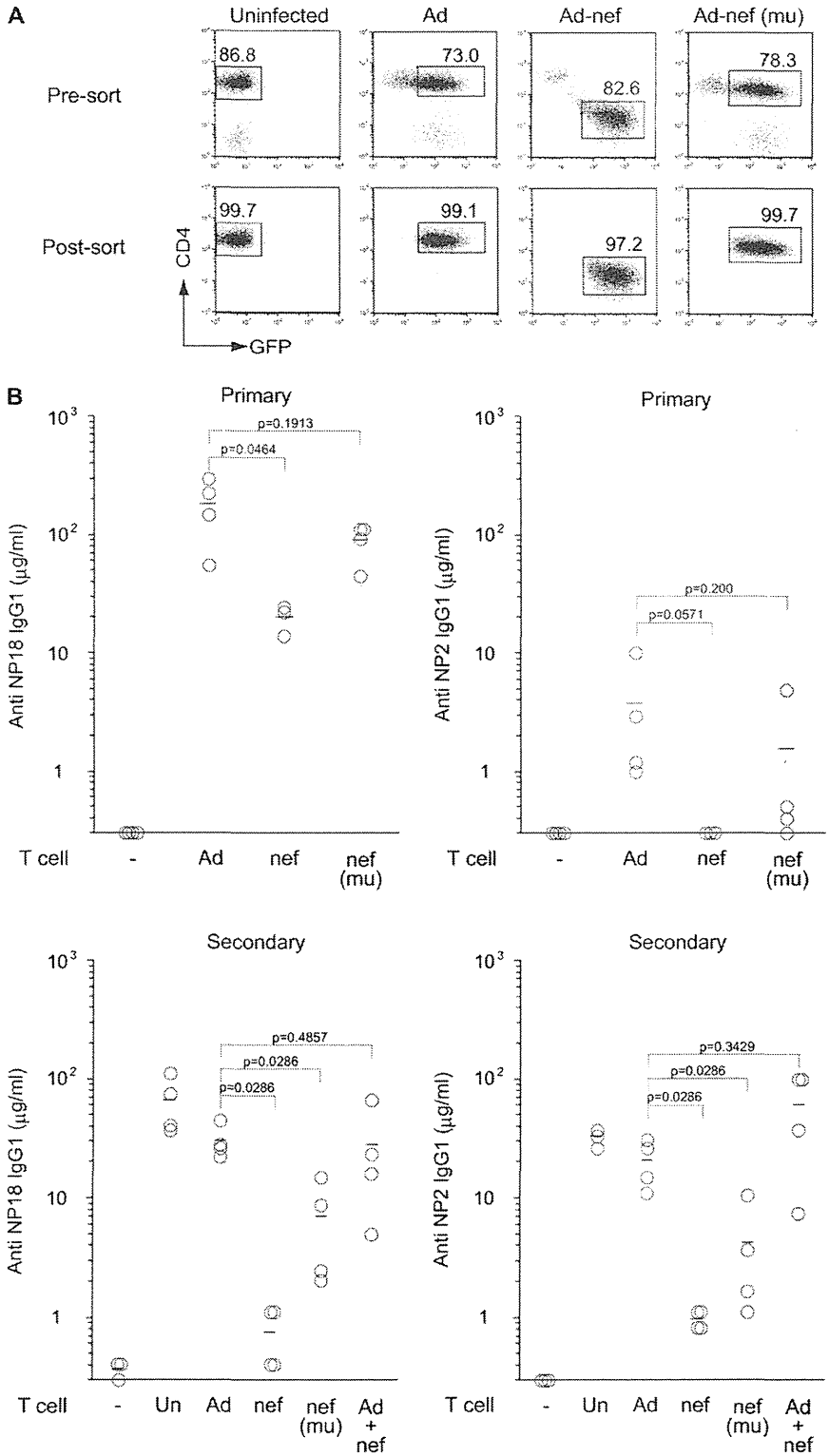

Fig. 3. Nef affects primary and memory B-cell response. (A) OVA-specific/CD4$^+$ T cells were purified from dTg mice and infected with Ad-nef, Ad-nef (mu) and Ad, followed by FACS purification (Post-sort). Numbers in plots indicate percent of GFP$^-$ uninfected cells and GFP$^+$ cells before (Pre-sort) and after purification (Post-sort). (B) Purified GFP$^+$ T cells (3×10^4) were transferred into CB17-scid mice, together with

with NP-OVA in alum for the primary response or soluble NP-OVA for the secondary response (Fig. 3B).

The results show that Nef expression in T cells reduced the level of anti-NP IgG1 serum antibodies by ~10-fold (NP_{18}; $P = 0.0464$, NP_2; $P = 0.0571$) in the primary response (Fig. 3B), whereas when the T cells were infected with Ad-Nef (mu), which does not down-regulate CD4 (Fig. 3A), the response was close to the control level (NP_{18}; $P = 0.1913$, NP_2; $P = 0.200$). As shown in Fig. 3(B), the impact of Nef on the secondary response was even more dramatic; there was a 30- to 40-fold reduction in both total and high-affinity anti-NP IgG1 antibodies (NP_{18}; $P = 0.0286$, NP_2; $P = 0.0286$). Reconstitution with equal numbers of non-infected and Nef-expressing OVA-specific $CD4^+$ T cells normalized the secondary adoptive response (NP_{18}; $P = 0.4857$, NP_2; $P = 0.3429$), excluding the possibility that Nef expression was generating suppressor T cells. Expression of the Nef mutant that was unable to down-modulate CD4 also reduced the secondary response (NP_{18}; $P = 0.0286$, NP_2; $P = 0.0286$), although the magnitude of the reduction was less than that induced by expression of wild-type Nef. These results demonstrate that Nef expression in peripheral T cells markedly diminishes their helper activity for the secondary IgG1 response and that this defect was only partially associated with the Nef-induced CD4 down-modulation. By contrast, this CD4 down-regulation appeared to be even more important for the reduced primary IgG1 response. These findings underscore the differential regulation in the primary and memory B-cell response. Thus, Nef affects helper T-cell activities in the primary and secondary response through different processes with different CD4 down-modulation susceptibility.

Discussion

In the present study, we have examined the consequence of Nef expression in primary splenic T cells. In order to avoid complications arising from expression of Nef early in T-cell development, e.g. lymphopenia, we established a double transgenic mouse (dTg), which expresses human CAR adenovirus receptor and an OVA-specific T-cell receptor that recognizes the OVA peptide on APC with high affinity under MHC Class II $I\text{-}A^d$-restriction. OVA-specific/$CD4^+$ T cells were purified from the spleen of dTg mice and infected with a recombinant adenovirus vector encoding Nef and GFP, followed by purification of GFP^+ cells using flow cytometry. To promote efficient introduction of the adenovirus vector into resting T cells, they were cultured for 2 days in the presence of the vector and IL-7, which is known to be important for survival of naive and memory T-cell populations (16). Neither naive nor memory $CD4^+$ T cells proliferate in response to IL-7, but they progress into the G_{1b} stage of the cell cycle (17). Thus, the present system allowed us to study the role of Nef in resting T cells in response to antigen-specific stimulation *in vitro* and *in vivo*.

During HIV-1 infection, the virus enters resting $CD4^+$ T cells and Nef is expressed even before the virus is integrated (1). It has been previously suggested that Nef expression in resting human T cells enhances IL-2 production upon activation by TCR cross-linking (1). This led to the proposal that Nef may enhance TCR signaling pathways that could help virus replication in partially stimulated T cells. In line with this viewpoint, it has been reported that Nef in human leukemic T cell lines and $CD4^+$ T-cell lines established from PBMC enhanced TCR signaling pathways and activated IL-2 production upon stimulation with TCR/CD28 or mitogens (2–5). In addition, Nef affects activation of murine T-cell hybridomas stimulated with anti-CD3 mAb (23), suggesting that the effect of Nef is not species specific.

In striking contrast, the present study demonstrates that Nef significantly reduces OVA-specific T-cell activation *in vitro* as defined by reduced proliferation and cytokine production, including IL-2 and IFNγ, but not completely. Furthermore, we demonstrate for the first time that Nef expression in OVA-specific resting T cells in the periphery reduced their ability to help anti-NP/$IgG1^+$ primary and secondary antibody responses in adoptive hosts after immunization with NP-OVA. In addition, in agreement with a previous *in vitro* analysis (7, 15), our *in vivo* results support the notion that Nef impairs the physiological recruitment of lymphocytes from the blood into the secondary lymphoid tissues after primary immunization, which promotes efficient antigen presentation and immune responses. Thus, Nef expressed in T cells at the early cell cycle stage impairs multiple functions in their subsequent antigen-specific response *in vivo*.

Why is the Nef-associated T-cell hyperresponse previously reported not detected in the present studies? The discrepancy does not reflect the differences in pathogenesis in *Nef* alleles (24) because the previous transgenic mouse models (8–10) and the present studies used the same NL4-3 Nef for characterization of the role of Nef protein in the immune system. Furthermore, the activation phenotype of T cells *in vitro* was induced by Nef proteins, irrespective of their alleles, including NL4-3 Nef (2–5). The discrepancy could be due to the cell state in the previous studies caused by transient over-expression of the protein in either the Jurkat T-cell line or in an activated human $CD4^+$ T-cell line established from PBMC (2–7). Another possible explanation is that previously reported assays utilized different TCR stimuli; the cells were stimulated by strong TCR ligation using immobilized antibodies (2–5). Such strong TCR ligation by antibodies forms stable TCR aggregates associated with the signaling complex (25). However, TCR stimulation with APC-presented antigen peptide forms an immunological synapse (IS) at the

B cells (5×10^6) which were enriched from the pooled spleens of either naive or 4-hydroxyl-3-nitrophenylacetyl-conjugated chicken γ-globulin (NP-CGG)-primed mice using a MACS system, followed by challenge with 100 μg of NP-OVA in alum (primary) or 25 μg of soluble NP-OVA (secondary). Serum anti-NP antibody titers were estimated by ELISA assays at day 7 after challenge using NP_2-BSA and NP_{18}-BSA as coating antigens. The relative affinity of anti-NP antibodies was estimated by calculating the ratio of anti-NP_2/anti-NP_{18} antibody. Representative data from two independent experiments is shown. Bars represent the mean of each group.

T-cell APC interface, facilitating signaling through TCR recognizing the peptide-loaded MHC molecules (26). The formation of IS was impaired *in vitro* by HIV-1 infection in a Nef-dependent manner (27), providing an explanation for the present results that Nef lowers the cognate interaction strength between T cells and APCs in antigen-specific response, thereby denying complete progression and activation of the cell cycle.

Nef affects helper T-cell activities in the primary and secondary response through different processes with different CD4 down-modulation susceptibility. However, the underlying mechanism remains obscure. In the B-cell response, antigen-activated helper T cells form a complex with B cells by interacting with several co-stimulatory molecules as well as with the TCR and peptide-loaded MHC class II molecules on B cells. As a consequence, T cells and B cells are mutually stimulated and T cells produce cytokines promoting B-cell proliferation and differentiation into antibody-forming cell (28). Therefore, it is likely that Nef-induced repression of T-cell helper activity for an antigen-specific B-cell response may also reflect an inefficient cognate interaction between T cells and B cells in the primary and secondary response.

We observed that Nef in resting murine $CD4^+$ T cells down-regulates the expression of CD4 on the cell surface, concordant with the previous results using human and murine T-cell lines (reviewed in ref. 1). It has been previously suggested that CD4 plays an important role in the activation of T cells by increasing the avidity of TCR for the peptide/MHC class II molecule and by transducing signals through the associated tyrosine kinase p56Lck (29). CD4 down-modulation significantly affects T-cell helper activity for the primary antibody response; however, it only partially affects T-cell helper function for the secondary response. On the other hand, Nef-mediated repression of antigen-specific T-cell function for the migratory capacity in the primary immune response is not the result of CD4 down-regulation. Thus, Nef affects multiple antigen-specific T-cell activities in the primary and secondary response through different processes with different CD4 down-modulation susceptibility, probably reflecting the T-cell signature and/or B-cell signature involved in the primary or the secondary antibody response.

CD4 binds to the MHC and boosts the recognition of ligand by the TCR in early T-cell activation, afforded by the IS formation (30) and functions to deliver Lck to the T-cell APC interface (31). However, signaling and co-stimulation later result in the movement of CD4 toward the periphery of the IS (30), suggesting that once Lck has been recruited to the synapse, the function of CD4 may become dispensable, allowing CD4 to leave the synapse, compatible with the idea that initial signal strength for T-cell activation may be crucial for the primary B-cell response. Nef might affect T-cell activity to form the IS with B cells, although, it remains unknown whether primary and memory B-cell responses require the same co-receptor molecules for T-cell interaction or if they need help from the same subset of T cells. Further analysis is needed to clarify how memory and naive B-cell responses are differentially regulated.

In summary, the present results support a model in which Nef expressing HIV-1 infected $CD4^+$ T cells fail to attain multiple functions required for normal immune responses. Thus, these combined effects of Nef may not facilitate extensive HIV-1 productions by increasing the numbers of productively infected cells through T-cell activations in antigen-specific immune response.

What could be the advantages for HIV-1 to inhibit proliferation and multiple T-cell functions required for immune response? Of note, Nef does not completely abrogate T-cell activation upon stimulation, as defined by expression of activated cell surface markers and a low level of cytokine production, which may allow a replicative advantage for the virus (reviewed in ref. 32). In activated $CD4^+$ T cells, viral replication is efficient and cytopathic (reviewed in ref. 32), though rapid death of infected cells may limit the production of the virus. By lowering the T-cell activity, Nef might facilitate a lowered level of viral spread and an increased infected T-cell life span by avoiding viral cytopathic effects. These cells may decay more slowly *in vivo* relative to activated cells, leading to vital consequences for the pathogenic outcome of infection in humans.

Supplementary data

Supplementary data are available at *International Immunology* Online.

Funding

This work was supported by a grant for Research on HIV/AIDS from the Ministry of Health, Labor and Welfare, Japan and in part by RIKEN (K94-34200 to T.T.).

Acknowledgements

We thank Drs Aya Isogai for constructing the nef (mu) plasmids and Peter Burrows for critically reviewing this manuscript and Ms Yoko Nakamura and Eri Watanabe for technical assistance.

References

1 Fackler, O. T. and Baur, A. S. 2002. Live and let die: Nef functions beyond HIV replication. *Immunity* 16:493.
2 Wang, J. K., Kiyokawa, E., Verdin, E. and Trono, D. 2000. The Nef protein of HIV-1 associates with rafts and primes T cells for activation. *Proc. Natl Acad. Sci. USA* 97:394.
3 Simmons, A., Aluvihare, V. and McMichael, A. 2001. Nef triggers a transcriptional program in T cells imitating single-signal T cell activation and inducing HIV virulence mediators. *Immunity* 14:763.
4 Manninen, A. and Saksela, K. 2002. HIV-1 Nef interacts with inositol trisphosphate receptor to activate calcium signaling in T cells. *J. Exp. Med.* 195:1023.
5 Fortin, J. F., Barat, C., Beausejour, Y., Barbeau, B. and Tremblay, M. J. 2004. Hyper-responsiveness to stimulation of human immunodeficiency virus-infected $CD4^+$ T cells requires Nef and Tat virus gene products and results from higher NFAT, NF-κB, and AP-1 induction. *J. Biol. Chem.* 279:39520.
6 Campbell, D. J., Kim, C. H. and Butcher, E. C. 2003. Chemokines in the systemic organization of immunity. *Immunol. Rev.* 195:58.
7 Janardhan, A., Swigut, T., Hill, B., Myers, M. P. and Skowronski, J. 2004. HIV-1 Nef binds the DOCK2-ELMO1 complex to activate rac and inhibit lymphocyte chemotaxis. *PLoS Biol.* 2:E6.
8 Hanna, Z., Kay, D. G., Rebai, N., Guimond, A., Jothy, S. and Jolicoeur, P. 1998. Nef harbors a major determinant of pathogenicity for an AIDS-like disease induced by HIV-1 in transgenic mice. *Cell* 95:163.
9 Rahim, M. M., Chrobak, P., Hu, C., Hanna, Z. and Jolicoeur, P. 2009. Adult AIDS-like disease in a novel inducible human immunodeficiency virus type 1 Nef transgenic mouse model:

$CD4^+$ T-cell activation is Nef dependent and can occur in the absence of lymphophenia. *J. Virol.* 83:11830.
10 Koenen, P. G., Hofhuis, F. M., Oosterwegel, M. A. and Tesselaar, K. 2007. T cell activation and proliferation characteristic for HIV-Nef transgenic mice is lymphopenia induced. *J. Immunol.* 178:5762.
11 Wan, Y. Y., Leon, R. P., Marks, R. *et al.* 2000. Transgenic expression of the coxsackie/adenovirus receptor enables adenoviral-mediated gene delivery in naive T cells. *Proc. Natl Acad. Sci. USA* 97:13784.
12 Murphy, K. M., Heimberger, A. B. and Loh, D. Y. 1990. Induction by antigen of intrathymic apoptosis of $CD4^+CD8^+TCR^{lo}$ thymocytes *in vivo*. *Science* 250:1720.
13 Kanegae, Y., Makimura, M. and Saito, I. 1994. A simple and efficient method for purification of infectious recombinant adenovirus. *Jpn. J. Med. Sci. Biol.* 47:157.
14 Takahashi, Y., Ohta, H. and Takemori, T. 2001. Fas is required for clonal selection in germinal centers and the subsequent establishment of the memory B cell repertoire. *Immunity* 14:181.
15 Choe, E. Y., Schoenberger, E. S., Groopman, J. E. and Park, I. W. 2002. HIV Nef inhibits T cell migration. *J. Biol. Chem.* 277:46079.
16 Marrack, P. and Kappler, J. 2004. Control of T cell viability. *Annu. Rev. Immunol.* 22:765.
17 Dardalhon, V., Jaleco, S., Kinet, S. *et al.* 2001. IL-7 differentially regulates cell cycle progression and HIV-1-based vector infection in neonatal and adult $CD4^+$ T cells. *Proc. Natl Acad. Sci. USA* 98:9277.
18 Craig, H. M., Pandori, M. W. and Guatelli, J. C. 1998. Interaction of HIV-1 Nef with the cellular dileucine-based sorting pathway is required for CD4 down-regulation and optimal viral infectivity. *Proc. Natl Acad. Sci. USA* 95:11229.
19 Dubey, S., Khalid, M., Wesley, C., Khan, S. A., Wanchu, A. and Jameel, S. 2008. Downregulation of CCR5 on activated CD4 T cells in HIV-infected Indians. *J. Clin. Virol.* 43:25.
20 Venzke, S., Michel, N., Allespach, I., Fackler, O. T. and Keppler, O. T. 2006. Expression of Nef downregulates CXCR4, the major coreceptor of human immunodeficiency virus, from the surfaces of target cells and thereby enhances resistance to superinfection. *J. Virol.* 80:11141.
21 Zajac, A. J., Blattman, J. N., Murali-Krishna, K. *et al.* 1998. Viral immune evasion due to persistence of activated T cells without effector function. *J Exp Med.* 188:2205.
22 Zhang, J. *et al.* 2000. Regulation of fas ligand expression during activation-induced cell death in T cells by p38 mitogen-activated protein kinase and c-Jun NH2-terminal kinase. *J. Exp. Med.* 191:1017.
23 Rhee, S. S. and Marsh, J. W. 1994. HIV-1 Nef activity in murine T cells. CD4 modulation and positive enhancement. *J. Immunol.* 152:5128.
24 Priceputu, E., Hanna, Z., Hu, C. *et al.* 2007. Primary human immunodeficiency virus type 1 nef alleles show major differences in pathogenicity in transgenic mice. *J. Virol.* 81:4677.
25 Bunnell, S. C., Hong, D. I., Kardon, J. R. *et al.* 2002. T cell receptor ligation induces the formation of dynamically regulated signaling assemblies. *J. Cell Biol.* 158:1263.
26 Dustin, M. L. 2009. The cellular context of T cell signaling. *Immunity.* 30:482.
27 Thoulouze, M. I., Sol-Foulon, N., Blanchet, F., Dautry-Varsat, A., Schwartz, O. and Alcover, A. 2006. Human immunodeficiency virus type-1 infection impairs the formation of the immunological synapse. *Immunity* 24:547.
28 Pereira, J. P., Kelly, L. M. and Cyster, J. G. 2010. Finding the right niche: B-cell migration in the early phases of T-dependent antibody responses. *Int. Immunol.* 22:413.
29 Veillette, A., Bookman, M. A., Horak, E. M., Samelson, L. E. and Bolen, J. B. 1989. Signal transduction through the CD4 receptor involves the activation of the internal membrane tyrosine-protein kinase p56lck. *Nature* 338:257.
30 Krummel, M. F., Sjaastad, M. D., Wulfing, C. and Davis, M. M. 2000. Differential clustering of CD4 and CD3ζ during T cell recognition. *Science* 289:1349.
31 Holdorf, A. D., Lee, K. H., Burack, W. R., Allen, P. M. and Shaw, A. S. 2002. Regulation of Lck activity by CD4 and CD28 in the immunological synapse. *Nat. Immunol.* 3:259.
32 Stevenson, M. 2003. HIV-1 pathogenesis. *Nat. Med.* 9:853.

Published October 1, 2012

JEM

Article

Distinct cellular pathways select germline-encoded and somatically mutated antibodies into immunological memory

Tomohiro Kaji,[1] Akiko Ishige,[1] Masaki Hikida,[6] Junko Taka,[1] Atsushi Hijikata,[2] Masato Kubo,[3] Takeshi Nagashima,[4] Yoshimasa Takahashi,[7] Tomohiro Kurosaki,[5] Mariko Okada,[4] Osamu Ohara,[2] Klaus Rajewsky,[8,9] and Toshitada Takemori[1]

[1]Laboratory for Immunological Memory, [2]Immunogenomics, [3]Signal Network, [4]Cellular Systems Modeling, and [5]Lymphocyte differentiation, RIKEN Research Center for Allergy and Immunology, Tsurumi, Yokohama, Kanagawa 230-0045, Japan
[6]Center for Immunoregulative Technology and Therapeutics, Graduate School of Medicine, Kyoto University, Sakyo-ku, Kyoto 606-8501, Japan
[7]Department of Immunology, National Institute of Infectious Diseases, Shinjyuku-ku, Tokyo 162-8640, Japan
[8]Program in Cellular and Molecular Medicine, Children's Hospital, and Immune Disease Institute, Harvard Medical School, Boston, MA 02115
[9]Immune Regulation and Cancer, Max-Delbrück-Center for Molecular Medicine, 13092 Berlin, Germany

One component of memory in the antibody system is long-lived memory B cells selected for the expression of somatically mutated, high-affinity antibodies in the T cell–dependent germinal center (GC) reaction. A puzzling observation has been that the memory B cell compartment also contains cells expressing unmutated, low-affinity antibodies. Using conditional Bcl6 ablation, we demonstrate that these cells are generated through proliferative expansion early after immunization in a T cell–dependent but GC-independent manner. They soon become resting and long-lived and display a novel distinct gene expression signature which distinguishes memory B cells from other classes of B cells. GC-independent memory B cells are later joined by somatically mutated GC descendants at roughly equal proportions and these two types of memory cells efficiently generate adoptive secondary antibody responses. Deletion of T follicular helper (Tfh) cells significantly reduces the generation of mutated, but not unmutated, memory cells early on in the response. Thus, B cell memory is generated along two fundamentally distinct cellular differentiation pathways. One pathway is dedicated to the generation of high-affinity somatic antibody mutants, whereas the other preserves germ line antibody specificities and may prepare the organism for rapid responses to antigenic variants of the invading pathogen.

CORRESPONDENCE
Toshitada Takemori:
mttoshi@rcai.riken.jp
OR
Klaus Rajewsky:
klaus.rajewsky@mdc-berlin.de

Abbreviations used: ASC, antibody-secreting cell; CG, chicken γ-globulin; CSR, class switch recombination; ES, embryonic stem; FO, follicular; GC, germinal center; MZ, marginal zone; NIP, (4-hydroxy-5-iodo-3-nitrophenyl)acetyl; NP, (4-hydroxy-3-nitrophenyl)acetyl; PNA, peanut agglutinin; qRT-PCR, quantitative RT-PCR; SHM, somatic hypermutation.

In T cell–dependent B cell responses, activated B cells migrate into the B cell follicles where they proliferate, with a fraction of cells undergoing Ig class switch recombination (CSR; Coffey et al., 2009; Pereira et al., 2010). Although some of the activated cells mediate the primary antibody response through differentiation into plasma cells, others are recruited into the germinal center (GC) reaction (Pereira et al., 2010). This is accompanied by up-regulation of the transcriptional repressor Bcl6, on which GC B cell differentiation depends (Dent et al., 1997; Ye et al., 1997). Bcl6 up-regulation is also required for the differentiation of follicular (FO) T helper (Tfh) cells. These cells are critical for the selection of B cells expressing high-affinity antibodies in the GC environment (Crotty, 2011).

Within the GC, B cells undergo massive proliferation accompanied by CSR and somatic hypermutation (SHM) of their rearranged Ig V region genes, a process in which cells preferentially survive which have acquired mutations that increase antibody affinity for the immunizing antigen (Rajewsky, 1996). This selection process critically depends on antigen presented to the B cells by FO DCs in the GC microenvironment and, in turn, presented by the B cells in the form of antigenic peptides to antigen-specific Tfh cells, resulting in the delivery of

The Rockefeller University Press $30.00
J. Exp. Med. 2012 Vol. 209 No. 11 2079-2097
www.jem.org/cgi/doi/10.1084/jem.20120127

Supplemental Material can be found at:
http://jem.rupress.org/content/suppl/2012/09/26/jem.20120127.DC1.html

Published October 1, 2012

JEM

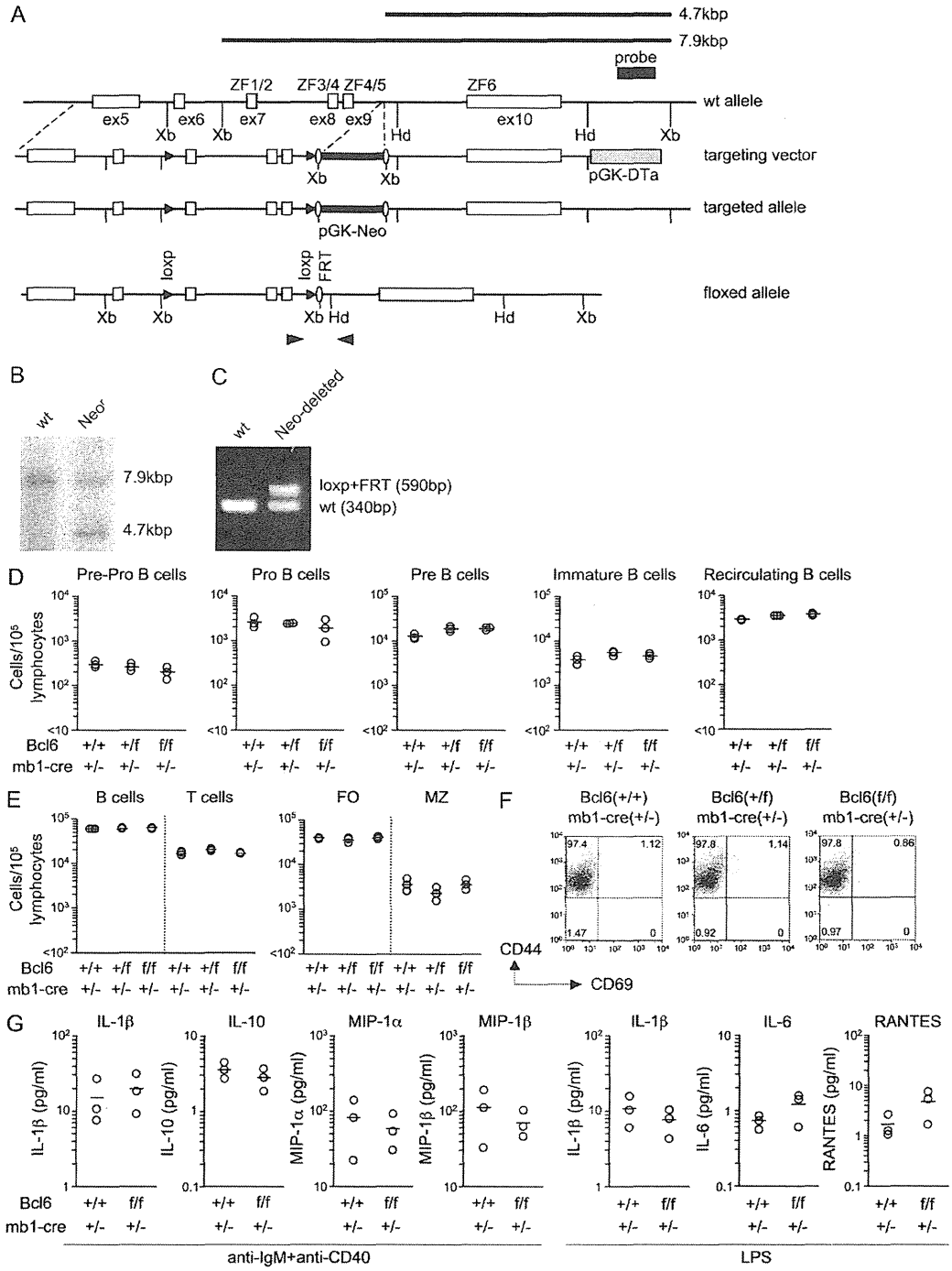

Figure 1. Targeted insertion of loxP sites into the *Bcl6* gene. (A). A DNA fragment which contains exons 7–9 of the *Bcl6* gene was flanked by *loxP* sites (solid triangles) with an FRT-flanked pGK-Neo cassette inserted next to it. The pGK-Neo cassette was removed from the mouse germline by breeding heterozygous mice to FLPe-expressing deleter mice. Xb, XbaI site; Hd, HindIII site. (B) Southern blot analysis of XbaI digested genomic DNA from a WT and a targeted ES clone using the probe depicted by the thick bar in A. (C) Removal of the pGK-Neo cassette in a heterozygous floxed mouse was confirmed by genomic PCR. Location of the primer set is indicated by the two arrowheads on the bottom of A. (D–G) $Bcl6^{flox}$ mice were crossed to *mb1*-cre mice. Conditional *Bcl6*-deletion in B cells does not affect BM B cell development (D), B cell numbers in the spleen (E), and B cell characteristics before immunization (F and G). BM cells and splenocytes were prepared from $Bcl6^{+/+}$ (+/+), $Bcl6^{+/f}$ (+/f), and $Bcl6^{f/f}$ (f/f) mice heterozygous for mb1-cre ($n = 3$). The frequency of B cell subsets in BM (D) and T and B cells in the spleen (E) was analyzed by FACS. Each symbol represents the number of cells in an individual mouse. Bars represent the mean number for

Published October 1, 2012

survival signals for the B cells involved (Victora et al., 2010). The selected high-affinity GC cells are then believed to differentiate into memory B and long-lived plasma cells, a large fraction of which express somatically mutated Ig V region genes and which persist for long periods of time after termination of the GC response (Rajewsky, 1996; Tarlinton, 2006).

Although the precursor-product relationship of GC and memory B cells seems firmly established, a puzzling observation has been that not all memory B cells carry somatic mutations in their Ig V regions (Takahashi et al., 2001; Blink et al., 2005; Anderson et al., 2007; Zotos et al., 2010). In addition, ICOS blockade early in the immune response caused a reduction in the frequency of mutated memory and GC B cells but did not affect total memory B cell numbers (Inamine et al., 2005). These findings led to the view that some memory cells emerge from the early GC reaction (Good-Jacobson and Shlomchik, 2010) or may even be GC independent, as unmutated memory cells can be generated in irradiated mice reconstituted with Bcl6-deficient BM (Toyama et al., 2002).

However, Bcl6 germline deletion causes multiple immunological dysfunctions, such as arrested Tfh and conventional DC development (Crotty, 2011; Ohtsuka et al., 2011), as well as aberrant macrophage function (Mondal et al., 2010). Furthermore, *Bcl6* germline deletion causes a prominent inflammatory disease owing to overexpression of Th2 cytokines (Ye et al., 1997; Dent et al., 1997) and affects the properties of B cells before immunization (Shaffer et al., 2000). Thus, there is no evidence for a GC-independent pathway of memory cell generation under physiological conditions. Moreover, even if such a pathway exists, its timing in the response and impact on B cell memory, and the properties of the participating cells remain elusive.

To obtain a comprehensive understanding of the population dynamics underlying GC-independent and -dependent memory B cell development under physiological conditions, we deleted Bcl6 in the B or T cell lineage through a conditional Bcl6 allele and complemented these experiments by antibody-mediated ablation of the GC response in genetically intact animals. Focusing on antigen-specific IgG1-expressing memory cells, which can be conveniently isolated and distinguished from GC B cells by the level of CD38 expression (Ridderstad and Tarlinton, 1998; Takahashi et al., 2001), we then pursued the fate of these cells in the T cell–dependent immune response and characterized their properties, genetic signature, life span, and functional activity.

Our work not only provides definitive evidence for a GC-independent pathway of memory cell generation under physiological conditions but also a comprehensive view of the strikingly distinct population dynamics underlying GC-independent and -dependent memory B cell development with the help of distinct T cell subsets. The two classes of memory cells establish the memory compartment jointly and at comparable frequencies and attain functional maturation through distinct though related transcriptional programs.

RESULTS

Bcl6 deletion in B cells impairs GC but not memory B cell development

We established mutant mice carrying a loxP-flanked *Bcl6* exon 7–9 allele ($Bcl6^{f/f}$), with these exons encoding the Bcl6 zinc finger (ZF) domains ZF1 to ZF5 (Fig. 1). As the ZF domains are critical for Bcl6 function (Basso and Dalla-Favera, 2010), deletion of exons 7–9 is predicted to cause a complete loss of the capacity of Bcl6 to repress transcription of target genes.

Whereas mice with *Bcl6* deletion in the germline exhibit aberrant B cell development in the BM and an activated phenotype in naive splenic B cells (Shaffer et al., 2000; Duy et al., 2010), the conditional deletion of *Bcl6* in B cells had no effect on B cell numbers, phenotype, or cytokine production after stimulation through the B cell receptor or Toll-like receptor (Fig. 1). To dissect IgG1 memory B cell development, $Bcl6^{f/f}$ mice were crossed with mice in which a cre cDNA is knocked into the *Cγ1* locus (Cγ1-cre; Casola et al., 2006). We immunized the compound mutants and control mice with chicken γ-globulin (CG) coupled to (4-hydroxy-3-nitrophenyl)acetyl (NP-CG) and tracked NP-specific/$IgG1^+$ memory ($CD38^+$/peanut agglutinin $[PNA]^{low}$) and GC ($CD38^{low}$/PNA^+) B cells in the spleen of immunized mice by multicolor flow cytometry (Fig. S1; Takahashi et al., 2001). GC reactions have been reported to persist for a long time after immunization (Dogan et al., 2009). Indeed, we found that approximately one fourth of the NP-specific/IgG1 B cells consisted of GC B cells 150 d after immunization (Fig. S1).

Bcl6 protein expression is limited to the GC stage of B cell differentiation (Basso and Dalla-Favera, 2010). Bcl6 was brightly stained in the nuclei of PNA^{high}/$CD38^+$ and $CD38^{dull}$ B cells at day 7 after immunization, supporting the notion that the transition of GC B cells from a $CD38^{high}$ to a $CD38^{dull}$ phenotype occurs early in the immune response (Shinall et al., 2000). Contrarily, Bcl6 was not detected in the nucleus of WT memory B cells (unpublished data). The conditional deletion of *Bcl6* reduced the number of NP-specific/$IgG1^+$ GC B cells in the spleen at days 7 and 40 after immunization to <2% of controls (Fig. 2 A). Early GC B cells were also deleted in the mutant mice (unpublished data). In striking contrast, the number of memory B cells was unaffected. These results suggest that Bcl6 expression in B cells is essential for GC but not memory B cell development.

To confirm this possibility, we crossed the $Bcl6^{f/f}$ mice with mice expressing Cre recombinase from the *mb-1* locus and thus from early on in B cell development (Hobeika et al., 2006). Cre-mediated recombination in WT mice was detected

each group. (F) Representative FACS plots of splenic B cells with expression of CD44 and CD69 (activated B cell phenotype). Numbers in the plots indicate the percentage of cells in quadrants. (G) The levels of cytokines in culture supernatants produced by splenic B cells upon stimulation with anti-IgM and anti-CD40 mAb or LPS for 3 d (see Materials and methods). Bars represent means for each group. The data are representative of two independent experiments in D–G.

Published October 1, 2012

JEM

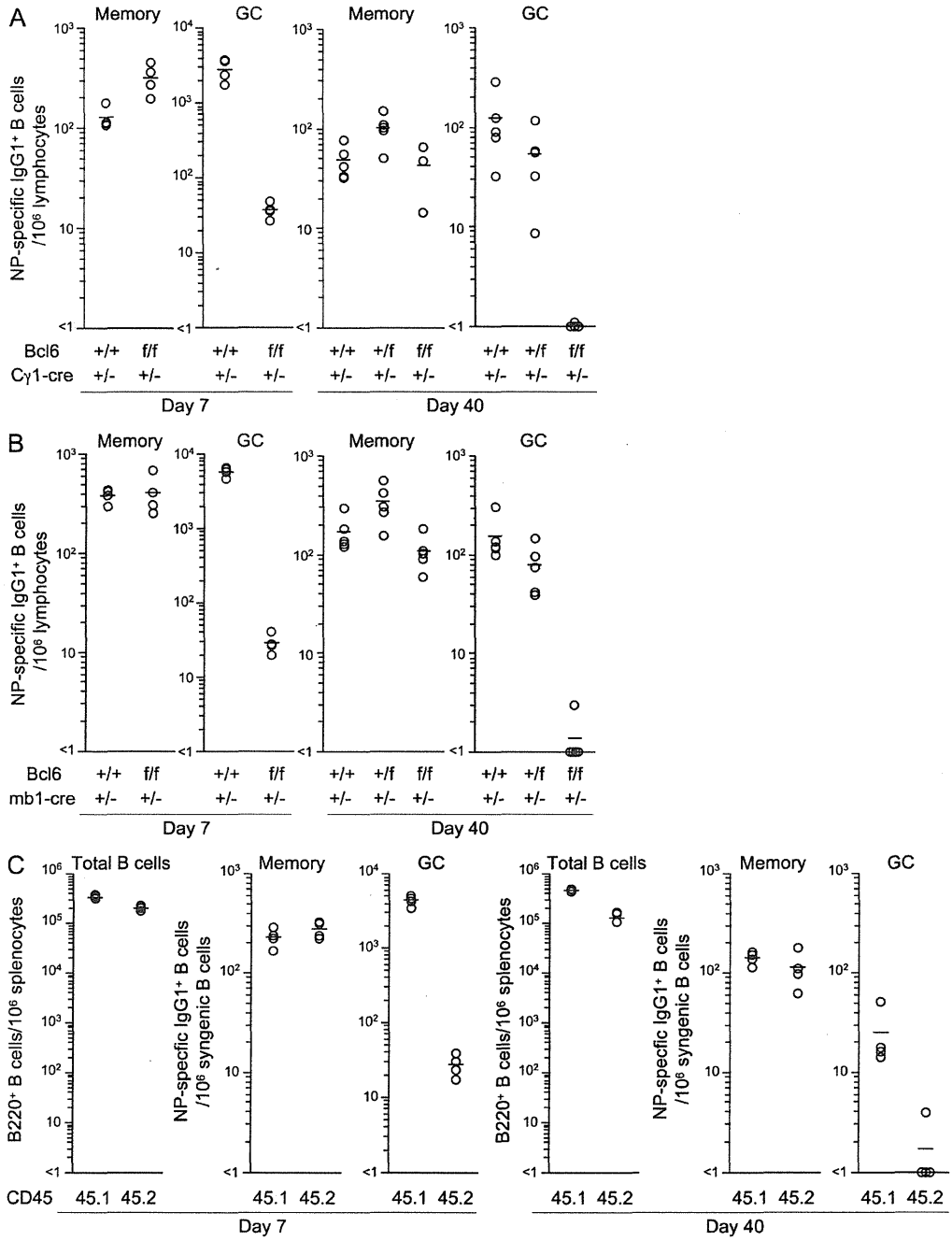

Figure 2. IgG1⁺ memory B cells develop independently of the GC reaction. Splenocytes were recovered from Bcl6$^{+/+}$, Bcl6$^{+/f}$, and Bcl6$^{f/f}$ mice heterozygous for Cγ1-cre (A) or mb1-cre (B) at day 7 or 40 after immunization with NP-CG in alum and NP-specific/IgG1⁺ memory and GC B cells were enumerated from 10^6 cells within the lymphocyte gate (see Materials and methods). Circles represent the number of cells in individual mice (n = 3–5). Bars indicate the mean number in each group. (C) BM cells from Bcl6$^{f/f}$ mice heterozygous for mb1-cre (CD45. 2⁺) and CD45.1⁺ WT or heterozygous mb1-cre mice were mixed 1:1 and transferred into CD45.2⁺Rag-1$^{-/-}$ mice (n = 4). After 8 wk, the recipient mice were immunized with NP-CG. Splenocytes were stained with anti-CD45.1 mAb to distinguish the WT (45.1) and conditional Bcl6 KO (45.2) compartments at days 7 and 40 after immunization. The number of B cells and NP-specific memory and GC B cells in individual spleens was determined as in A. Data are representative of two (A) and three (B and C) independent experiments. See also Fig. S1.

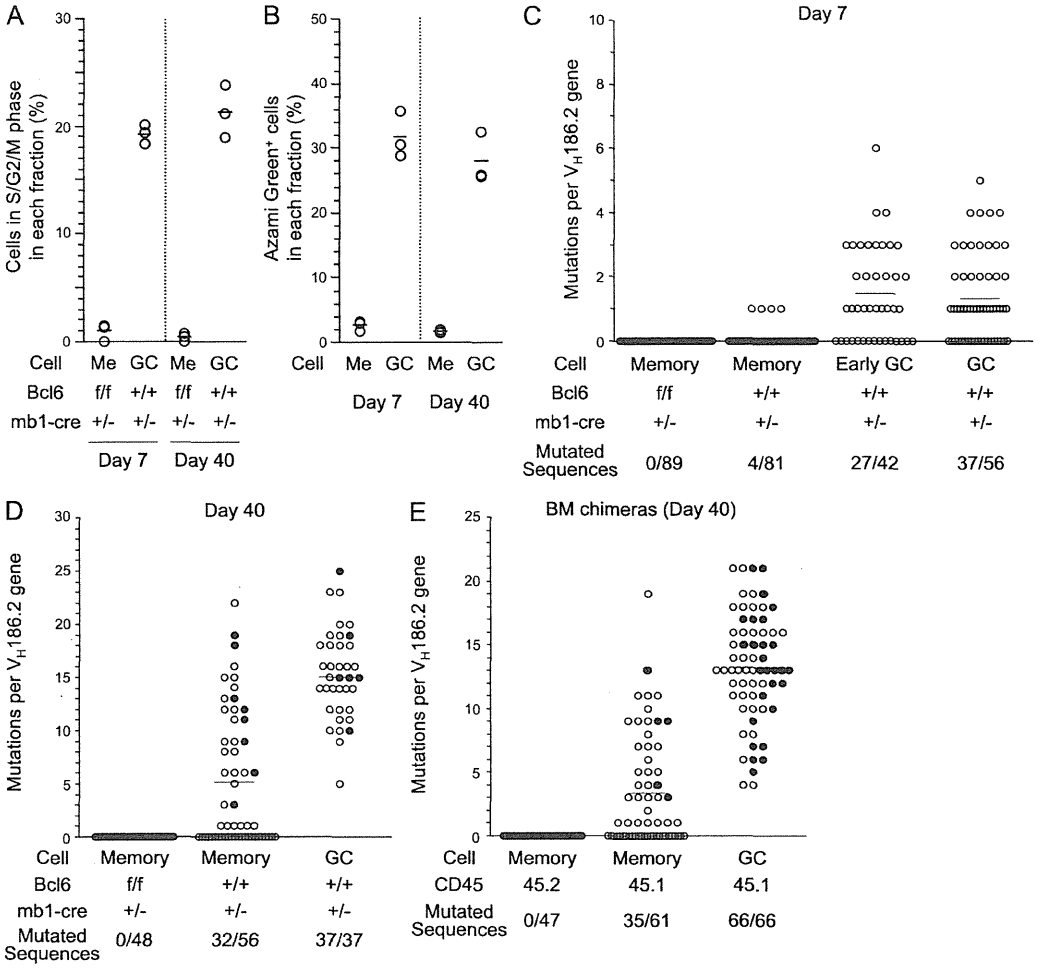

Figure 3. The cell cycle position and V_H186.2 gene mutations in NP-specific memory and GC B cells. (A) DNA content in memory (Me) and GC B cells in conditional Bcl6-deficient ($Bcl6^{f/f}$/mb-1-$cre^{+/-}$) and control ($Bcl6^{+/+}$/mb-1-$cre^{+/-}$) mice at days 7 and 40 after immunization with NP-CG. Each symbol represents the percentage of positive cells in an individual mouse ($n = 3$). Data are representative of three independent experiments. (B) The cell cycle position of memory B cells (Me) and GC B cells (GC) in FUCCI transgenic mice ($n = 3$) at indicated times. Each symbol represents the percentage of cells positive for Azami Green in an individual mouse. Data are representative of three (day 7) and two (day 40) independent experiments. (C and D) Single NP-specific/IgG1$^+$ memory and GC B cells were purified from the pooled spleens of $Bcl6^{+/+}$ (+/+) and $Bcl6^{f/f}$ (f/f) mice heterozygous for mb1-cre ($n = 6$–13) at day 7 (C) or day 40 (D) after immunization and subjected to RT-PCR to amplify rearranged *V_H186.2-Cγ1* cDNA for sequencing (see Materials and methods). (E) CD45.1$^+$ (45.1) WT memory and GC B cells and CD45.1$^-$ (45.2) Bcl6-deficient memory B cells were purified as single cells from pooled spleens of BM chimeras ($n = 9$) at day 40 after immunization and their V_H genes were sequenced as in C. Number of mutated clones/number of V186.2 genes sequenced are also shown in C–E. Circles represent the number of mutations in individual clones. Closed circles represent W33L clones.

in >98% of BM and splenic B cells, but not in prepro–B and CD4$^+$ T cells (unpublished data). The conditional deletion of *Bcl6* through mb1-cre essentially abolished the early development of IgG1$^+$ GC B cells in the spleen on day 5 after immunization (unpublished data). This in turn resulted in an ~200-fold reduction in the number of GC B cells on day 7 after immunization, compared with the controls (Fig. 2 B). We also generated mixed BM chimeras by transferring BM cells of congenic CD45.1$^+$ WT and CD45.2$^+$ conditional Bcl6-deficient mice into irradiated Rag-$1^{-/-}$ mice and immunized the animals with NP-CG 8 wk after reconstitution. In the chimeric mice, Bcl6-deficient B cells did not generate GC B cells (Fig. 2 C), confirming that Bcl6 expression in B cells is essential for GC B cell development.

In contrast, the number of IgG1$^+$ memory B cells was again comparable in *Bcl6*-deficient ($Bcl6^{f/f}$/mb1-$cre^{+/-}$) and control mice ($Bcl6^{+/+}$/mb1-$cre^{+/-}$) at days 7 and 40 after immunization (Fig. 2 B). In BM chimeric mice, memory B cells derived from WT and conditional Bcl6-deficient mice coexisted at almost equal frequency in the spleen (Fig. 2 C), suggesting that GC-dependent and -independent pathways of memory cell generation operate side by side.